ROBUST CONCATENATED CODES FOR THE SLOW RAYLEIGH FADING CHANNEL

A Thesis

by

TEH-HSUAN HSU

Submitted to the Office of Graduate Studies of
Texas A&M University
in partial fulfillment of the requirements for the degree of

MASTER OF SCIENCE

May 2008

Major Subject: Electrical Engineering

ROBUST CONCATENATED CODES FOR THE SLOW RAYLEIGH FADING CHANNEL

A Thesis

by

TEH-HSUAN HSU

Submitted to the Office of Graduate Studies of
Texas A&M University
in partial fulfillment of the requirements for the degree of

MASTER OF SCIENCE

Approved by:

Chair of Committee,	Krishna R. Narayanan
Committee Members,	Jean-Francois Chamberland
	Jim Ji
	Prabir Daripa
Head of Department,	Costas N. Georghiades

May 2008

Major Subject: Electrical Engineering

ABSTRACT

Robust Concatenated Codes For The Slow Rayleigh Fading Channel. (May 2008)

Teh-Hsuan Hsu, B. En, National Chiao Tung University, Hsinchu, Taiwan

Chair of Advisory Committee: Dr. Krishna R. Narayanan

In this thesis, we design a robust concatenated code for the Multiple-Input Multiple-Output (MIMO) system in the presence of slow Rayleigh fading with no channel side information at the transmitter (no CSIT) and perfect channel side information at the receiver (perfect CSIR). Since we are interested in the slow fading channel, outage capacity is used as the measure of performance. Good space-time codes can be designed so as to maximize the so-called rank and the determinant criteria. However, a practical system will concatenate a space-time code with an outer code at the transmitter and perform iterative decoding at the receiver. It is necessary to design the space-time code together with the outer code in practice. We will call this kind of code a concatenated space-time code.

At the transmitter, we will consider the bit-to-symbol mapping and space-time code together as a space-time modulator and thus, Bit Interleaved Coded Modulation (BICM) and Multilevel coding (ML) can be applied to design outer codes for the non-binary constellation. However, the concatenated space-time codes designed by these two methods can only be decoded with arbitrarily small error probability for a fixed channel realization and such designs are not robust over the ensemble of fading channels.

Our approach of designing concatenated space-time code is to design an outer code for a space-time modulator such that the concatenated space-time code can be decoded with arbitrarily small error probability in a set of fixed channels which have the same capacity. Through this approach, we discovered a new design criterion for space-time codes: a good space-time code should stabilize its Extrinsic Information Transfer (EXIT) charts. In other words, the robustness of a space-time code in the slow fading channel and its performance in iterative decoding can be visualized by the EXIT charts.

The rank and the determinant criterion do not evaluate the performance of a space-time code in iterative decoding, but the new criterion does. Therefore, the new criterion is applicable to design concatenated space-time codes.

Applying our approach and new criterion, a rate 7.2 bits/s/Hz concatenated space-time code is designed. The performance is close to the outage capacity, and the rate lost is 0.2 bits/s/Hz.

TABLE OF CONTENTS

CHAPTER Page

LIST OF FIGURES

FIGURE Page

FIGURE Page

FIGURE Page

CHAPTER I

INTRODUCTION

In wireless communication, a transmitted signal will experience a multiplicative noise, or fading gain which is usually represented as a random variable in an equivalent baseband model. For example, the Rayleigh fading can be modeled as the fading gain being a complex Gaussian random variable with zero mean and unit variance. A common way of exploiting the randomness of the channel is to employ multiple antennas at the transmitter and the receiver, also called a multiple-input and multiple-output (MIMO) system. A MIMO system can transmit a signal through multiple paths, which enables the receiver to average out a bad received signal. This phenomenon is called diversity gain, and can be quantified as the rate of decay of the probability of error at the receiver as a function of the signal-to-noise ratio (SNR). In the MIMO system, it is possible to obtain a maximum diversity gain equal to the number of transmit antennas multiplied by the number of receive antennas.

For a communication system with no channel side information at the transmitter (CSIT) and full channel side information at the receiver (CSIR), in order to achieve the maximum or full diversity gain in a MIMO system, the transmitter needs to transmit the signal in a carefully designed way. This can be done by the space-time modulator of the transmitter. The space-time modulator maps the vector of binary data into the vector of complex numbers and then places the complex numbers into a series of matrices named codewords of the space-time code. For a space-time codeword, the number of row vectors represents the number of transmit antennas and the number of column vectors represent the number of time instances needed to transmit a codeword. Conventionally, the performance of a space-time modulator is evaluated by its diversity and coding gain: good space-time code not only provides both full diversity gain in a MIMO system and coding gain. These two quantities can be evaluated by the rank and determinant criteria.

This thesis follows the style of IEEE *Transactions on Information Theory*.

At the transmitter in a practical communication system, a concatenated space-time code which is a space-time modulator concatenated with a binary outer encoder is used to provide more protection to the data. At the receiver, the decoder is separated into two stages, space-time demodulator and outer decoder which are iteratively used. Therefore, designing a practical MIMO system must consider the space-time modulator together with the outer encoder. However, the rank and the determinant criteria do not evaluate the performance of a space-time code in iterative decoding and there is no criterion for designing concatenated space-time codes in previous studies.

In this thesis, we are interested in designing a MIMO system in the slow Rayleigh fading channel with no CSIT and perfect CSIR. We propose a new criterion for designing concatenated space-time codes. This new design criterion can be represented in terms of the Extrinsic Information Transfer (EXIT) chart, which is a tool for analyzing the behavior of a code with iterative decoding.

Chapter II first establishes the discrete time model for a MIMO system in the slow Rayleigh fading channel. Based on this model, the outage capacity and the diversity gain are also introduced. Section 2.2 presents two conventional space-time code design criteria and three space-time codes represented by the discrete time model.

In Chapter III, the concatenated coding scheme and iterative decoding of concatenated codes are introduced. The space-time modulator is taken as the inner code of a concatenated code; hence, we can use the concatenated code design tool to analyze the behavior of space-time modulator with iterative decoding. Section 3.3 presents the EXIT chart as a tool to study the behavior of inner and outer codes in iterative decoding. The method of designing a concatenated code by the EXIT chart is also presented in this section.

Chapter IV first shows two coding methods, Bit Interleaved Coded Modulation and Multilevel Coding, for non-binary constellations. The concatenated space-time codes designed by these two methods are not robust in a slow fading channel. Then we introduce our design criterion represented by the EXIT chart. We further design a concatenated space-time code for the 2x2 MIMO system by applying this new criterion

with multilevel coding. The 2x2 MIMO system performs close to the outage capacity with a very small rate-loss.

CHAPTER II

MIMO CHANNEL AND SPACE-TIME CODE

In this chapter, we first introduce a discrete time model for the Multiple Input Multiple Output (MIMO) channel with slow Rayleigh fading, with channel state information unknown at the transmitter (no CSIT) and perfectly known at the receiver (perfect CSIR). Capacity and diversity gains are also presented in this section. These terms quantify the ability and the efficiency of a system to communicate through a MIMO channel with arbitrarily small error probability at the receiver. Following the MIMO channel section, space-time codes will be discussed. We first show the design criteria for space-time codes, and then the Vertical Bell-Labs Layered Space Time code (VBLAST) and space-time codes based on number theory are introduced. We will evaluate these space-time codes by applying the design criteria. Finally we show the performances of these space-time codes in the slow Rayleigh fading channel through simulation.

2.1 MIMO Channel

A point to point communication system with M_t transmit antennas and M_r receive antennas is shown in Figure 2.1. The received signal can also be represented using the following discrete time model:

$$\begin{bmatrix} y_{1,1} & \cdots & y_{1,T} \\ \vdots & \ddots & \vdots \\ y_{Mt,1} & \cdots & y_{Mt,T} \end{bmatrix} = \begin{bmatrix} h_{1,1} & \cdots & h_{1,Mt} \\ \vdots & \ddots & \vdots \\ h_{Mr,1} & \cdots & h_{Mr,Mt} \end{bmatrix} \begin{bmatrix} x_{1,1} & \cdots & x_{1,T} \\ \vdots & \ddots & \vdots \\ x_{Mt,1} & \cdots & x_{Mt,T} \end{bmatrix} + \begin{bmatrix} n_{1,1} & \cdots & n_{1,T} \\ \vdots & \ddots & \vdots \\ n_{Mt,1} & \cdots & n_{Mt,T} \end{bmatrix} \tag{2.1}$$

or simply as

$$Y_k = \sqrt{\frac{\rho}{2}} H X_k + N_k, \quad k = 1, 2 \ldots L \tag{2.2}$$

were X_k is the transmitted symbols (or a codeword) represented by a matrix with M_t rows and T columns, T is the number of time instances required to transmit X_k, $h_{i,j}$ is the channel gain from transmit antenna i to receive antenna j and is a complex zero-mean, unit variance Gaussian random variable, N_k is the Gaussian noise represented by a column matrix with M_r i.i.d. complex zero-mean unit variance Gaussian random variables as its elements and H is a $M_r \times M_t$ matrix whose entries are $h_{i,j}$. Note that we call the channel a Rayleigh fading channel because of the statistical properties of $h_{i,j}$. Since (2.2) is a discrete time model, k is the index for transmitted symbols and L is the number of transmitted codewords. The constant ρ is the received signal to noise ratio (SNR) at each receive antenna. H is kept constant for the entire L transmissions in our discussion; in addition, we assume H is not known at the transmitter and is fully known at the receiver.

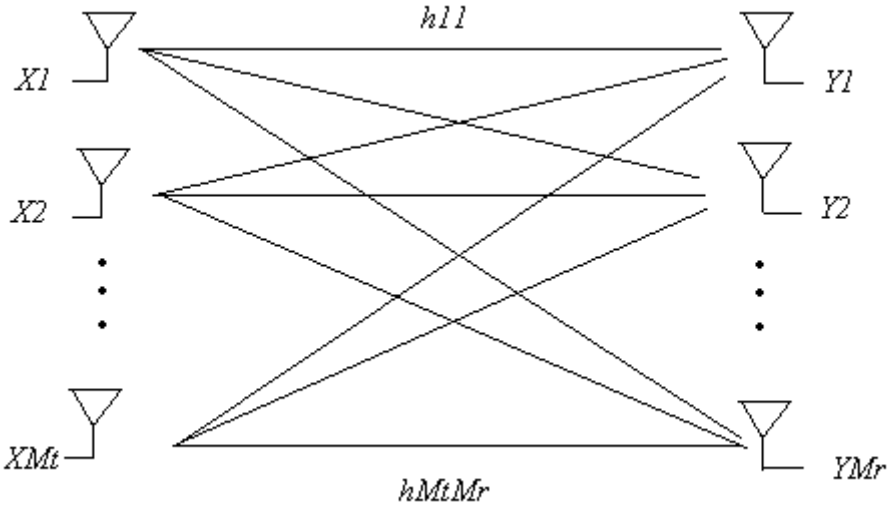

Fig.2.1: MIMO systems

2.1.1 Capacity of MIMO Channel

Capacity is defined as the maximum rate at which the data can be transmitted through a channel with arbitrarily small error probability, assuming no constraints on delay or complexity of the encoder and decoder. It is the maximum mutual information between transmitted symbol X and received symbol Y:

$$C = \max_{p(x)} I(X;Y) = \max_{p(x)} [H(Y) - H(Y \mid X)] \quad \text{bits/s/Hz} \tag{2.3}$$

where by definition, H($Y|X$) is equal to the entropy of Gaussian noise H(N), therefore, maximizing mutual information is equivalent to maximizing H(Y). From [1] and [2], (2.3) is equal to the following mutual information:

$$C = \max_{R_x : Tr(R_x) = \rho} \log_2 \det[\mathrm{I}_{Mr} + HR_xH^H] \quad \text{bits/s/Hz} \tag{2.4}$$

where R_x is the covariance matrix of $\mathbf{X}$ and the optimization relative to R_x will depend on whether or not H is known or not at the transmitter.

If H is known at the transmitter, the water-filling method which allocates power across antennas ideally can be applied to maximize (2.4). However, since we consider a MIMO system with no CSIT and perfect CSIR, we will assume H is not known at the transmitter. Hence, the transmitter cannot change the data rate since it does not know the channel at all, thus the transmitter will transmit data at a fixed rate R (bits/s/Hz). We are interested in the slow fading channel where H is fixed over time but random. Therefore, we consider non-ergodic channels in this case and the appropriate definition of capacity is capacity with outage. The outage capacity associated with R is the probability that the channel H can only support a data rate less than R, so the received data can have arbitrarily small error probability. This probability is given by

$$P_{out}(R) = p\left(\max_{R_x : Tr(R_x) = \rho} \log_2 \det[\mathrm{I}_{Mr} + HR_xH^H] < R \right) \tag{2.5}$$

Outage is an important idea for understanding other properties of MIMO channels. This will be seen in the following sections.

With no CSIT, the transmitter cannot maximize (2.4) by optimizing its power allocation or input covariance structure across antennas. Intuitively, the best strategy should be transmitting signals with equal power in each antenna. It is shown in [3] that with no CSIT and perfect CSIR, uniform power allocation across antennas maximizes the mutual information of the i.i.d. Rayleigh slow fading MIMO channel. With uniform power allocation, the covariance matrix is an identity matrix times a constant: $R_x = (\rho/M_t)I_{Mt}$. Thus, we can rewrite (2.5) as follows:

$$P_{out}(R) = p(\log_2 \det[I_{Mr} + \frac{\rho}{M_t} HH^H] < R) \tag{2.6}$$

where ρ is the signal to noise ratio (SNR) at each antenna of the system.

The capacity of the MIMO channel with no CSIT and perfect CSIR depends on the specific realization of the matrix H, in particular its singular values or eigenvalues. If the slow fading case is being considered, the channel gain matrix H in (2.2) is constant during the entire transmission (H is constant from k = 1 to k = L). Therefore, the left hand side of the inequality in (2.6) is the exact capacity for the MIMO channel H. Chapter IV will introduce an approach, where by the channel realizations of the i.i.d. slow Rayleigh fading channel can be drawn under a fixed channel capacity. In addition, the outage capacity is the measure of performance for the system we designed.

2.1.2 Diversity Gain

For a communication system, we can approximate its bit error rate (BER) of received signal as a function of the SNR of the channel

$$BER \approx C \times \rho^{-D} \tag{2.7}$$

where the diversity gain D is the negative exponent of SNR and C is the coding gain. We can say that diversity gain determines how fast the bit error rate of a communication system decreases with increase in SNR.

Diversity gain comes from the fact that a symbol being transmitted between transmitter and receiver experiences multiple channel realizations. For example, in a

single-input single-output system (SISO), the diversity gain depends on the number of channel realizations that the transmitted symbol experiences during the transmission. In a MIMO system, diversity gain can be achieved by transmitting a symbol over multiple antennas through the channel. In the slow fading channel, the maximum diversity gain of a MIMO system, shown in Fig.2.1, is $M_r \times M_t$. The easiest way to achieve maximum diversity gain is repetition coding where X_k in (2.2) is a diagonal matrix and $x_{1,1} = x_{2,2} = \ldots = x_{Mt,Mt} = x$. However, this is not an efficient way to transmit the data since only one symbol, x, is transmitted in Mt time instances. In order to gain efficiency (data rate) and reliability (diversity and coding gain) at the time, space-time codes can be applied.

2.2 Space-time Codes

For a MIMO system, the transmitted signal can be designed for both diversity and coding gains. When the signal design extends over both space (via antennas) and time (via multiple symbol time intervals), it is typically referred to as a space-time code.

Most space-time codes, including the codes discussed in the following sections, are designed for quasi-static channels, where the channel is constant over a block of symbol time intervals and the channel is assumed to be unknown at the transmitter. Therefore, the discrete time MIMO channel model shown in (2.1) and (2.2) is a valid model so the transmitted signal encoded by a space-time code and the received signal can be written as matrices in (2.1).

In the following sections, we first discuss the design criteria for space-time codes. Thus, we can have a standard to evaluate different space-time codes; then, the VBLAST, a space-time code based on number theory and the Golden Code for 2×2 MIMO channel will be discussed after the design criteria.

2.2.1 Design Criteria for Space-time Code

The MIMO systems and space-time codes were invented in order to improve the data rate and/or the reliability of communication. The question now is how to design a space-time code such that the MIMO system can have low bit error rate at the receiver. Tarokh et al's work [5] provides the answer for this question. In [5], there are two design criteria for space-time codes being designed for slow Rayleigh fading channel. The rank criterion quantifies the diversity gain and the determinant criterion quantifies the coding gain.

1 *The Rank Criterion*: For a space-time code of $m \times n$ MIMO channel to achieve the maximum diversity gain $m \times n$, it has to be designed such that the difference matrix $B(\mathbf{X_1}, \mathbf{X_2})$ between any two codewords $\mathbf{X_1}$, $\mathbf{X_2}$ from the space-time code has full rank equal to min(m,*n)*. If the minimum rank is r ($r < n$), then a diversity gain $r \times m$ is achieved.

2 *The Determinant Criterion*: A high coding gain is achieved by maximizing the minimum of the determinant of the matrix $A(\mathbf{X_1}, \mathbf{X_2}) = B(\mathbf{X_1}, \mathbf{X_2})\, B^*(\mathbf{X_1}, \mathbf{X_2})$ over all codewords.

2.2.2 Space-time Code: VBLAST

VBLAST is also known as spatial multiplexing. The received signal can be written as (2.2), where $T = 2$ and $\mathbf{X}_k$ is a 2×2 matrix whose entries $\mathbf{x}_1$, $\mathbf{x}_{2,}$ $\mathbf{x}_3$ and $\mathbf{x}_4$ can be chosen from the same signal constellation (ex: M-QAM, M-PSK…). The structure of VBLAST for 2×2 MIMO channel is shown in Fig. 2.2.

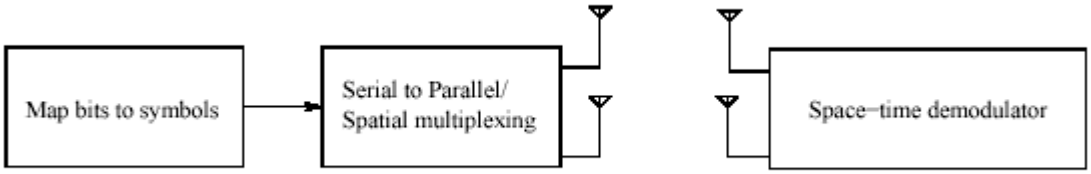

Fig.2.2 VBLAST for 2×2 MIMO channel

At the encoder, the binary data are mapped onto some constellation (ex: M-QAM, M-PSK…), and then multiplexed onto two transmit antennas. The overall rate is, therefore, $2log_2M$ bits per channel used if M-QAM is used. A 2×2 MIMO system with VBLAST can achieve at most a diversity gain of two, because each symbol is transmitted by one transmit antenna and received by two receive antennas.

At the receiver, if the successive cancellation algorithm is used, receiver complexity can be reduced significantly. However, receiver complexity is not addressed in this thesis; thus, the maximum likelihood decoder is used in the receiver, and the actual decoder algorithm will be discussed in detail in the next chapter.

2.2.3 Space-time Code Based on Number Theory

One way to design a space-time code is to apply number theory, as presented in [16]. Full data rate linear dispersion space-time block codes (LD-STBC) over two transmit antennas and two time instances are also presented in [16]. Unlike VBLAST, this space-time code achieves a full transmit diversity of two over all constellations chosen from Z[i]. For a 2×2 MIMO wireless communication system, a space-time code so designed can achieve full diversity of four.

Based on the MIMO channel model (2.1) and (2.2), the space-time code presented in [16] can be written as

$$X_k = \frac{1}{\sqrt{2}} \begin{bmatrix} s_1 + \phi s_2 & \theta(s_3 + \phi s_4) \\ \theta(s_3 - \phi s_4) & s_1 - \phi s_2 \end{bmatrix} \tag{2.8}$$

where $\theta^2 = \phi$ and $\phi = e^{i\lambda}$, such that λ is a real parameter to be optimized. The information symbols s_1, s_2, s_3 and s_4 are modulated from binary data using QAM or PAM.

A space-time code, as in (2.8), can transmit four information symbols in two time intervals, which means two information symbols being transmitted in one time interval. The rate is $2log_2M$ bits per channel used which is the same with VBLAST if M-QAM is used. In a 2×2 MIMO system, this is actually the best rate we can obtain if M-QAM is used; therefore, a space-time code like (2.8) is a full-rate code for 2×2 MIMO systems.

In order to satisfy the design criteria mentioned in 2.2.1, ϕ has to be chosen carefully to maximize transmit diversity and coding gains. It is shown in [16] that if ϕ is an algebraic number of degree $\geqq 4$ over Q(i) then one guarantees the maximum transmit diversity over all constellations chosen from Z[i]. If the information symbols are modulated by 4-QAM, the maximum transmit and coding gain is attained for $\phi = e^{i/2}$ and the coding gain is 0.2369. For the 16-QAM case, the maximum transmit and coding gain is attained for $\phi = e^{0.521i}$ and the coding gain is 0.0591. In the following contents, we are going to call the LD-STBC with optimized ϕ as LD codes. Note that the coding gain decreases when the size of the constellation increases and the determinant will vanish when the size of the constellation goes to infinity. This property is also shown in [16].

The space-time codes introduced in this section are full rate and full diversity codes for a 2×2 MIMO system. They can be optimized to satisfy the design criteria mentioned in 2.2.1. However, the problem is that the vanishing determinant will decrease the coding gain when the size of the constellation increases.

At the receiver, the maximum likelihood decoder is used and will be discussed in detail in the next chapter.

2.2.4 Space-time Code: Golden Code

The Golden Code is a space-time block code for the 2×2 MIMO wireless communication system. It was presented by Belfiore [6] in 2005. The Golden Code is also a member of the LD-STBC family. The received signal can also be written as (2.1) and (2.2) except the codewords $\mathbf{X}_k$ of the Golden Code are 2×2 complex matrices of the following form:

$$X_k = \frac{1}{\sqrt{5}}\begin{bmatrix} \alpha(s_1 + s_2\theta) & \alpha(s_3 + s_4\theta) \\ i\sigma(\alpha)(s_3 + s_4\sigma(\theta)) & \sigma(\alpha)(s_1 + s_2\sigma(\theta)) \end{bmatrix} \tag{2.14}$$

where s_1, s_2, s_3 and s_4 are information symbols which can be taken from any M-QAM constellation carved from Z[i]. $\theta = (1+\sqrt{5})/2$ is the "Golden number" which gives the name of this space-time code, $\sigma(\theta) = 1-\theta$, $\alpha = 1+i\sigma(\theta)$ and $\sigma(\alpha) = 1+i\theta$.

Same as the space-time code introduced in 2.2.3, the Golden Code can transmit four information symbols in two time intervals, which means two information symbols being transmitted in one time interval. The rate of the Golden Code is also $2log_2$M bits per channel used if M-QAM is used; therefore, the Golden Code is also a full-rate code for 2×2 MIMO systems.

Besides full rate, the Golden Code has other properties which satisfy the design criteria for Rayleigh space-time code, as proposed by Tarokh [5]. First, the Golden Code is full-rank, which means that the determinant of the difference between two different codewords is always nonzero [5] [7]. This property can guarantee that the Golden Code will achieve a maximum diversity of four.

Second, the Golden Code has a non-vanishing determinant for increasing rate (increasing M in M-QAM case). In fact, the minimum determinant is defined as

$$\delta_{\min}(C_\infty) = \min_{X \in C_\infty, X \neq 0} \left|\det(X)\right|^2 \tag{2.15}$$

where C_∞ is the set of codewords when rate goes to infinity and is equal to 1/5 from [6]. By [5], this property can guarantee that the Golden Code will have a nonzero coding gain as rate increases which means $\delta_{\min}$ of the Golden Code does not depend on the size of the signal constellation.

In contrast, other full rank and full-rate space-time codes, like the space-time code introduced in 2.2.3, have nonzero minimum determinants of C_∞, but determinants vanish as the spectral efficiency of the signal constellation is increased. The non-vanishing determinant may pique our interest because in an actual communication system, one may employ different signal constellations in order to explore spectral efficiency. Therefore, space-time codes with a lower bounded non-vanishing determinant can always guarantee the system having coding gain no matter which signal constellation is employed.

For a finite rate Golden Code, the minimum determinant is the following:

$$\delta_{\min}(C) = \min_{X_1, X_2 \in C, X_1 \neq X_2} \left|\det(X_1 - X_2)\right|^2 \tag{2.16}$$

where C is the set of the codewords of the Golden Code. It can be shown that the minimum determinant has a lower bound:

$$\delta_{\min}(C) \geq 16\delta_{\min}(C_\infty) = \frac{16}{5} \tag{2.17}$$

which satisfies the sufficient condition for achieving the optimal diversity-multiplexing tradeoff [8]. Therefore, the Golden Code provides optimal diversity-multiplexing tradeoff in a 2×2 MIMO system and satisfies the determinant criterion because of the non-vanishing determinant.

As explained in [6], the performance improvement not only comes from the non-vanishing δ_{min} but also comes from the fact that the constellation of Golden Code is a rotated version of $Z[i]^2$, As such, there is no shaping loss in the signal constellation emitted by the transmit antennas.

At the receiver, the sphere decoder can be employed in order to reduce the decoder complexity. However, as the decoder of VBLAST, the maximum likelihood decoder is employed in this thesis and the decoder algorithm will be discussed in detail in the next chapter.

2.3 Comments

Conventionally, space-time codes can be evaluated by the rank and determinant criteria. VBLAST is not full rank, the minimum rank of its difference matrices is one, and thus VBLAST does not achieve the maximum diversity of a MIMO system. In a 2×2 MIMO system, VBLAST can achieve the diversity gain of two at most. On the other hand, the LD codes and the Golden Code are full rank which means that they can achieve a diversity gain of four in a 2×2 MIMO system.

VBLAST does not have nonzero δ_{min} and cannot guarantee the coding gain and the LD codes in 2.2.3 do not have a lower bound for its decreasing determinant. However, the Golden Code has the non-vanishing nonzero δ_{min}, thus guaranteeing the coding gain with any signal constellation.

Figure 2.3 shows the frame error rate of VBLAST, LD codes and Golden Code in 2×2 slow Rayleigh fading channel with no CSIT and perfect CSIR. The maximum likelihood decoder is applied for all space-time codes.

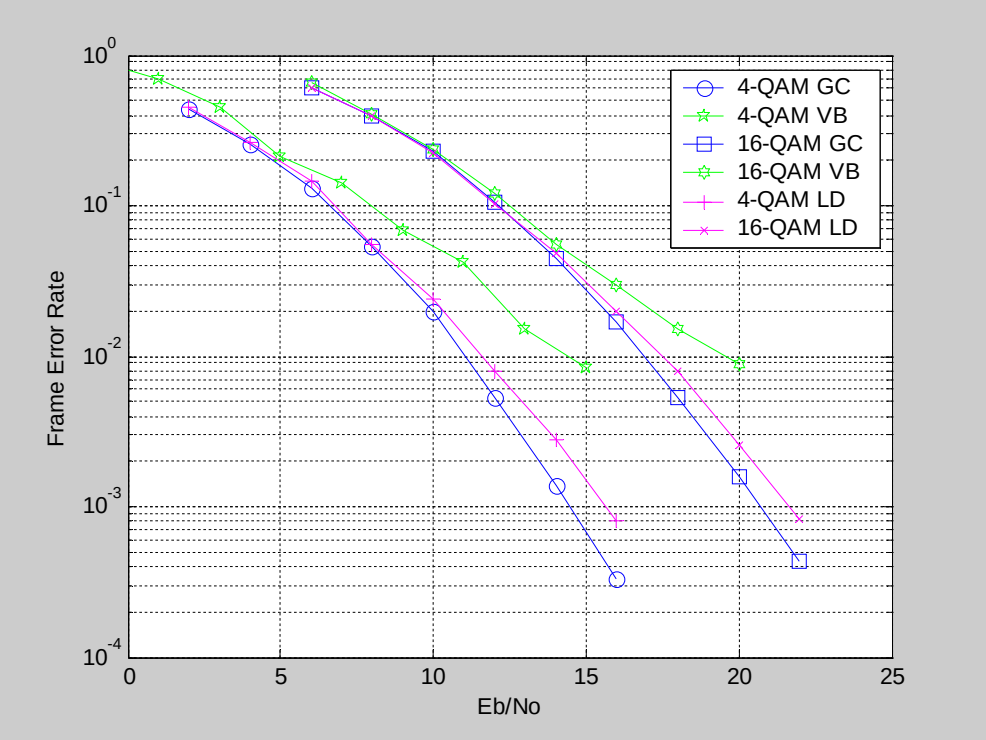

Fig.2.3 Frame error rate for space-time codes in slow Rayleigh fading

From the simulation, it can be seen that the performances of VBLAST are significantly different from the other two codes at high bit to noise ratio because it does not achieve full diversity. The performance difference at high signal to noise ratio between the Golden Code and the LD codes comes from the fact that the Golden Code has minimum determinant 16/5, as shown in (2.17) for any constellation size and is always larger than the minimum determinant of LD codes[6]. This results in the Golden Code always having better coding gain than the LD codes.

Although we went through the properties and the actual performances of three particular space-time codes, there is still not much information about their robustness in a practical MIMO system. For a practical system, the space-time code will be concatenated with an outer code, while the method of designing a space-time code and an outer code together is unanswered in this chapter and proposed in Chapter IV.

CHAPTER III

CONCATENATED CODES

Concatenated codes are composed of two levels of codes: an outer code and an inner code, as shown in Fig.3.1.

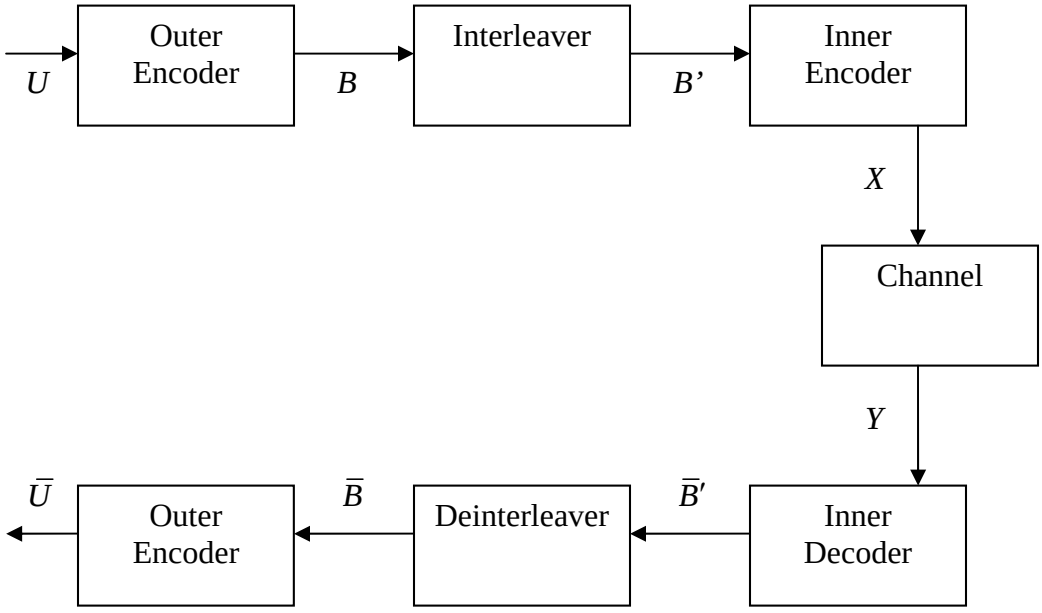

Fig.3.1 Concatenated coding

Usually the inner code is designed to correct most of the errors caused by the channel, and the outer code further corrects the errors which cannot be corrected by the inner code. Concatenated codes have the following properties: first, they are particularly effective when the channel is in deep fades. Second, they typically achieve very low error probability with less complexity than a single code with the same error probability performance.

The optimal decoder for the concatenated code is the maximum likelihood decoder which performs joint decoding; however, this is a high complexity decoder and is not practical. A practical way to implement the decoder is to decode in two stages, as shown in Fig.3.1: first the received signal Y is decoded by the inner decoder, and then $\overline{B}$ is decoded by the outer the decoder. This is a suboptimal decoder since the separated the inner and outer decoders can only use the information contained in the inner code and outer code, respectively. In the mid-90's, the idea of iterative decoding was introduced and will be shown in the next section.

In the following sections, we will introduce serial concatenated codes whose inner codes are the space-time modulators discussed in the previous chapter and outer codes are low-density parity-check (LDPC) codes. Once the iterative decoding is performed, we need a decoding model and a tool to analyze the behavior of each space-time code (inner code).

3.1 Serial Concatenated Codes and Decoding Model

The serial concatenated codes model for a 2×2 slow Rayleigh fading channel is shown in Fig.3.2 and can be represented by (2.2) where H is a 2×2 matrix whose entries are complex Gaussian random variables with zero mean and unit variance. Note that there is no interleaver and deinterleaver in Fig.3.2, since we utilize LDPC codes for the outer code. At the transmitter, the vector of binary data U will be encoded by the outer encoder. The vector of encoded binary data B will be mapped to QAM symbols and then mapped into matrices as codewords shown in (2.1) and (2.2). X is a vector whose elements are X_k in (2.2); similarly, Y is a vector whose elements are Y_k in (2.2). The double-headed arrow between the space-time demodulator (decoder) and outer decoder represents the iterative decoding performed between these two decoders.

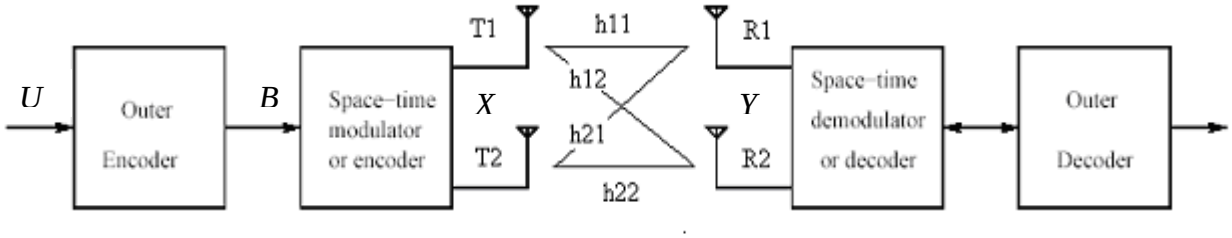

Fig.3.2 A serial concatenation model with 2 transmit antennas and 2 receive antennas

3.1.1 Iterative Decoding

Iterative decoding was first invented for decoding turbo codes which is a kind of parallel concatenated code [9], [10]. The idea of using log-likelihood algebra is that the two decoders are soft-in/soft-out decoders that accept and pass the log-likelihood ratios of the codewords iteratively as inputs and outputs [11]. Because log-likelihood ratios are passed, the term "soft" is used in order to contrast with hard decision decoding.

First, the space-time decoder will process the received signal to generate a vector of "a posteriori" likelihood values (L-values) for each element in *B*, then the vector of "a posteriori" L-values is passed to the outer decoder as its "a priori" L-values A_{out} as shown in Fig.3.3. Next, the outer decoder processes A_{out} to generate a vector of "extrinsic" L-values E_{out}, then passes it back to the space-time decoder as "a priori" L-values A_{ST}. Together with the received signal and A_{ST}, the space-time decoder generates a vector of "extrinsic" L-values E_{ST} which is equal to the vector of "a posteriori" L-values minus A_{ST} and is passed to the outer decoder as its new A_{out}. This iterative process which is shown (see Fig.3.3) continues until the L-values reach a point such that the "average extrinsic information" converges to a value.

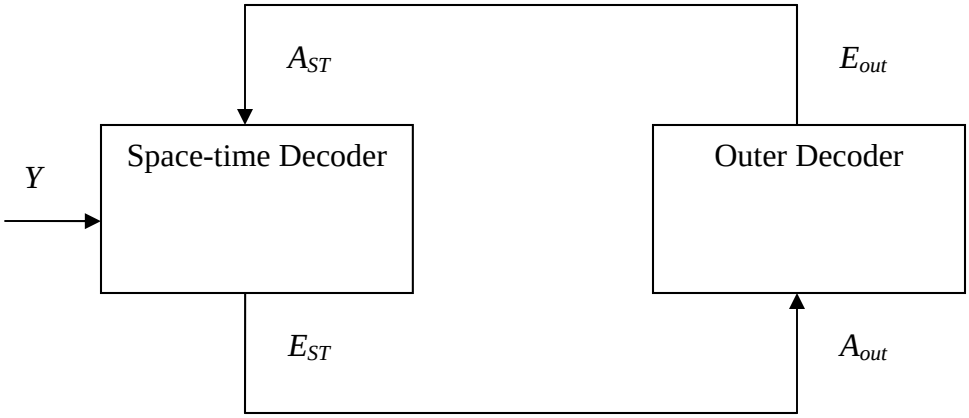

Fig.3.3 Iterative decoding

From Fig.3.3, it can be seen that the space-time decoder has to process the received signal and A_{ST} together to generate E_{ST}. The optimum bit wise a posteriori probabilities (APP) decoder is used to process the received signal and A_{ST} together. In the next section, a decoding model for APP decoding will be presented.

3.1.2 Decoding Model for Space-time Decoder

In [12], a decoding model for parallel and serial concatenated codes is presented (see Fig.3.4). The source randomly produces a binary data vector U of k independent information bits each taking on values 0 and 1 with probability 1/2. Note that k is the number of information bits contained in one space-time code word; for example if the Golden Code with a 4QAM constellation is used for the space-time code, k is equal to 8 (4 information symbols, each contains 2 information bits). In the model in Fig.3.2, the source can be the outer encoder, which is the LDPC encoder, as mentioned before. X is the codeword of the space-time code and is a 2×2 matrix. B is a vector of the modulated U, the elements are 1 or -1. The decoder receives two vectors: a noisy version Y of X and a noisy version B' of B.

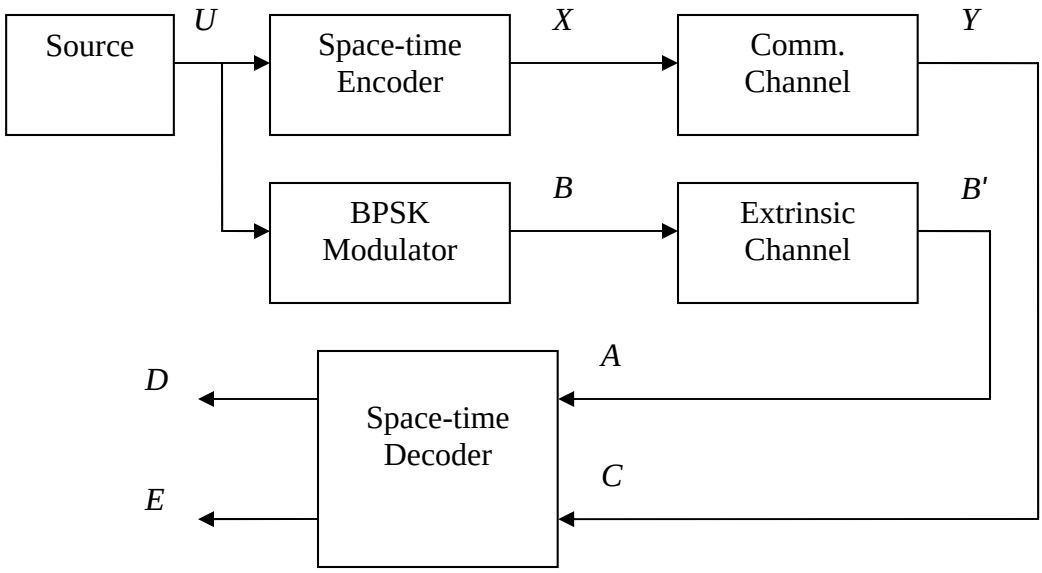

Fig.3.4. A decoding model for parallel and serial concatenated codes

The communication channel is the 2×2 slow Rayleigh fading channel, therefore the relationship between *X* and *Y* can be modeled as in (2.2). On the other hand, the extrinsic channel is used to model the a priori L-values from the outer decoder. *B′* is used as if it was a priori information from the outer decoder. The extrinsic channel, which is assumed to be a memoryless channel, is used to observe the behavior of the space-time decoder in iterative decoding. Note that in actual concatenated codes, *B′* comes from the output of the outer decoder.

At the space-time decoder, two inputs, *Y* and *B′*, are used as two estimates of data source *U*: the a posteriori L-values *D* and the extrinsic L-values *E*. The output of the extrinsic channel *B′* gives a priori information about the data source *U*, with L-values

$$a_i = \log \frac{P(b'_i \mid u_i = 0)}{P(b'_i \mid u_i = 1)}, \; i = 1, 2 \ldots k \qquad (3.1)$$

where a_i represents the elements of vector *A*, b'_i the elements of vector *B′* and u_i the elements of vector *U*. The a priori L-values a_i can be thought of as the “extra” information which comes from an imaginary extrinsic channel about the information bit u_i. In concatenated codes, this “extra” information is provided by the outer decoder and

will be processed together with the information coming from the actual communication channel. With the assumption that the extrinsic channel is an AWGN channel, equation (3.1) can be written as

$$a_i = \log \frac{\exp(-\frac{\|b_i - 1\|^2}{2\sigma^2})}{\exp(-\frac{\|b_i + 1\|^2}{2\sigma^2})}, \; i = 1, 2 \ldots k \qquad (3.2)$$

or

$$a_i = \frac{-1}{2\sigma^2}(\|b_i - 1\|^2 - \|b_i + 1\|^2), \; i = 1, 2 \ldots k \qquad (3.3)$$

where σ is the standard deviation of the AWGN channel. Similarly the output of the communication channel Y gives information about the data source *U*, with L-values

$$c_i = \log \frac{P(Y \mid u_i = 0)}{P(Y \mid u_i = 1)}, \; i = 1, 2 \ldots k \qquad (3.4)$$

where c_i represents the elements of vector *C*. Obviously, (3.4) is the information about the information bit u_i given by the communication channel.

The space-time decoder is an APP decoder that computes the a posteriori L-values *D*

$$d_i = \log \frac{P(u_i = 0 \mid Y, B')}{P(u_i = 1 \mid Y, B')}, \; i = 1, 2 \ldots k \qquad (3.5)$$

where d_i is the element of vector *D* and P(u_i=0 | Y, B') is the probability that the source data $u_i = 0$ is conditioned on the received signal *Y* and the a priori information *B'*. From (3.5), the a posteriori L-value can be viewed as the information about the information bit u_i given the information from the communication and extrinsic channels. For further analysis, we write U_i for the vector *U* with the *i*th entry removed, i.e., $U_i = [u_1\ u_2 \ldots u_{i-1}\ u_{i+1} \ldots u_k]$. The numerator of equation (3.5) can be rewritten as

$$P(u_i = 0 \mid Y, B') = \sum_{U_i : u_i = 0} P(U_i \mid Y, B') = \sum_{U_i : u_i = 0} \frac{P(Y, B' \mid U_i) P(U_i)}{P(Y, B')}, \quad i = 1, 2 \ldots k \tag{3.6}$$

Applying (3.6) to (3.5) and using the fact that Y and B' are conditional independent of U_i, the a posteriori L-values are

$$d_i = \log \frac{\sum_{U_i : u_i = 0} P(B' \mid U_i) P(Y \mid U_i)}{\sum_{U_i : u_i = 1} P(B' \mid U_i) P(Y \mid U_i)}, \quad i = 1, 2 \ldots k \tag{3.7}$$

where the conditional probabilities $P(B` \mid U_i)$ and $P(Y \mid U_i)$ are nothing but the probabilities of the a priori information $B`$ and the received signal Y given a data source vector U_i. Note that the space-time encoder and BPSK modulator both perform one-to-one mapping; therefore, equation (3.7) can also be written as

$$d_i = \log \frac{\sum_{U_i : u_i = 0} P(B' \mid B_i) P(Y \mid X_i)}{\sum_{U_i : u_i = 1} P(B' \mid B_i) P(Y \mid X_i)}, \quad i = 1, 2 \ldots k \tag{3.8}$$

where B_i is U_i modulated using BPSK and X_i is U_i encoded by the space-time encoder. This result shows that the a posteriori L-value d_i comes from marginalizing all combinations of extrinsic information $B`$ and the information from the communication channel for a given information bit u_i. With the assumption that the extrinsic channel is an AWGN channel and the receiver has perfect knowledge of the communication channel, (3.8) can be rewritten as

$$d_i = \log \frac{\sum_{U_i : u_i = 0} \exp\left(\frac{-\left\| B' - B_i \right\|^2}{2\sigma_e^2} + \frac{-\left\| Y - HX_i \right\|^2}{2\sigma_c^2}\right)}{\sum_{U_i : u_i = 1} \exp\left(\frac{-\left\| B' - B_i \right\|^2}{2\sigma_e^2} + \frac{-\left\| Y - HX_i \right\|^2}{2\sigma_c^2}\right)}, \quad i = 1, 2 \ldots k \tag{3.9}$$

where σ_e and σ_c are the standard deviations for the extrinsic channel and the communication channel respectively. These two factors will determine the effects of

extrinsic information and channel information on the a posteriori value. The better the channel (extrinsic or communication) quality is, the bigger the effect of the channel on the a posteriori value. This will be the APP decoder for our space-time decoder and will be applied through all simulations in this thesis. Note that although we have thought of the extrinsic channel as being an AWGN channel, this is not required. We can directly use the LLR provided by the outer decoder. However, we use the AWGN channel here to make it consistent with the EXIT chart section discussed later, where we will assume that these LLR have a Gaussian distribution.

We showed that the numerator of the a posteriori L-value d_i in (3.5) can be expanded to derive the mathematical expression for the APP decoder; however, it can also be expanded in a way to show the relationship between the incoming information (*A* and *C*) and outgoing information (*D* and *E*). Such expansion is shown below:

$$\begin{aligned} & P(u_i = 0 \mid Y, B^{'}) \\ &= \sum_{U_i : u_i = 0} P(U_i \mid Y, B^{'}) \\ &= \sum_{U_i : u_i = 0} \frac{P(Y \mid U_i, B^{'}) P(B^{'} \mid U_i) P(U_i)}{P(Y, B^{'})} \\ &= \sum_{U_i : u_i = 0} \frac{P(Y \mid X_i) P(B^{'} \mid B_i) P(U_i)}{P(Y, B^{'})} \\ &= \frac{P(b_i^{'} \mid u_i = 0)}{P(Y, B^{'})} \cdot \sum_{U_i : u_i = 0} P(U_i) P(B_i^{'} \mid B_i) P(Y \mid X_i) \end{aligned} \quad , i = 1, 2 \ldots k \quad (3.10)$$

where the last step follows if the extrinsic channel is memoryless. The denominator of (3.5) can also be expanded in the same way and inserting the results into (3.5), we have

$$d_i = a_i + e_i \, , \; i = 1, 2 \ldots k \quad (3.11)$$

where

$$\begin{aligned} e_i &= \log \frac{P(u_i = 0 \mid Y, B_i^{'})}{P(u_i = 1 \mid Y, B_i^{'})} \\ &= \log \frac{\sum_{U_i : u_i = 0} P(B_i^{'} \mid B_i) P(Y \mid X_i)}{\sum_{U_i : u_i = 1} P(B_i^{'} \mid B_i) P(Y \mid X_i)} \end{aligned} \quad , i = 1, 2 \ldots k \quad (3.12)$$

The value e_i is called the extrinsic L-value about b_i or u_i. It can be viewed as the information about the *i*th information bit given by the communication channel, as well as the extrinsic information about all information bits except for the *i*th information bit. From (3.12), the extrinsic L-value can also be viewed as the increasing amount of information about the information bit u_i that comes from the APP decoder. This extrinsic information will be sent to the outer decoder as a priori information. After the outer decoder processes this information, it will also generate the extrinsic information which will be sent to the APP decoder as a priori information. This process will continue iteratively until the average extrinsic information for both decoders converges. Note that it is the extrinsic L-values instead of the a posteriori L-values being passed between two decoders. This is because the extrinsic L-values are the result of the a priori L-values being subtracted from the a posteriori L-values. This avoids the propagation of the inputted a priori information which is the information already possessed by the decoder. The iterations proceed until a stopping critierion is satisfied when the iterations can be stopped. There are several stopping criteria that are commonly used and they are not discussed in this thesis.

Although iterative decoding and its decoding model are presented, a tool to model the iterative behavior between the space-time decoder and the outer decoder is still necessary. In the next section, the EXIT functions and EXIT charts are introduced as tools to analyze and design the concatenated codes.

3.2 EXIT Functions and EXIT Charts

In iterative decoding, as discussed in previous sections, the space-time decoder and the outer decoder perform an iterative process with a vector of soft information being passed between two decoders. At the beginning, Gallager [14] suggested evaluating the convergence behavior of iterative decoders for LDPC codes by tracking the probability distributions of extrinsic L-values. This is a simple procedure for erasure channels because only the fraction of erasures is passed between inner decoder and outer decoder. However, for other channels, the entire probability density function must be tracked. This procedure is called density evolution. For channels, which we are studying, it is difficult to analyze the vector of soft information being passed between two decoders using density evolution.

However, tenBrink introduced a very useful tool in his work [13]: the Extrinsic Information Transfer (EXIT) chart. Rather than tracking the probability density function, another way to evaluate the convergence behavior of iterative decoders is to track only one number per iteration. For example, one might track a statistic of the extrinsic L-values such as their mean, variance, an error probability or mutual information. In [12], the EXIT functions are defined to describe the relationship between the input and output average mutual information of a decoder and the EXIT charts illustrate the EXIT functions. Several reasons for using EXIT charts are listed in [12].

- Mutual information seems to be the most accurate statistic.
- Mutual information is the most robust statistic, in the sense that it applies without change to the widest range of channel modulations and detectors. For instance, EXIT functions apply to ECs without change.
- EXIT functions have analytic properties with useful implications for designing codes and iterative processors.

These are very useful properties of EXIT charts, especially the last claim. The area property introduced in [12] will be examined in this chapter and will be used to show that the design of concatenated codes is just a curve-fitting problem.

3.2.1 Average a priori and extrinsic information

In order to track the a priori and extrinsic L-values by using one statistic, [12] suggests using the average mutual information defined as the following:

$$I_A = \frac{1}{k}\sum_{i=1}^{k} I(u_i; a_i) \tag{3.13}$$

$$I_E = \frac{1}{k}\sum_{i=1}^{k} I(u_i; e_i) \tag{3.14}$$

where k is the length of information bits of the data source U, u_i is an element of U and e_i and a_i are entries of E and A defined in (3.12) and (3.1) respectively. The value I_A is called the average a priori information going into the decoder, and I_E is called the average extrinsic information coming out of the decoder. An EXIT function is defined so that I_E can be described as a function of I_A and an EXIT chart will plot I_E as a function of I_A. Note that u_i is chosen from 0 or 1 with equal probability 1/2 and I_A and I_E are averages of mutual information, thus $0 \leqq I_A, I_E \leqq 1$. When I_A or I_E equals one, the decoder has full knowledge of data U and can decode it with arbitrarily small error probability.

These two quantities are important measurements for inputs and outputs of a decoder. Notice that the output extrinsic information from a decoder is a function of the input a priori information. This relationship can be expressed in terms of a transfer function (EXIT function) for each decoder, namely $T_{in}(I_A)$ and $T_{out}(I_A)$. Note that $T_{in}(I_A)$ is usually a function of the channel fading gain and signal to noise ration also. Iterative decoding starts with the inner decoder receiving no a priori information and then sends the extrinsic information, whose average mutual information is $T_{in}(0)$, to the outer decode. The outer decoder takes the extrinsic information of the inner decoder as its a

priori information and then generates the extrinsic information whose mutual information is $T_{out}(T_{in}(0))$. The extrinsic information generated by the outer decoder is sent to inner decoder as its a priori information. This process continues iteratively until the mutual information of the decoder's output converges to a fixed point.

The iterative decoding described above can be shown easily by an EXIT charts. With the help of the properties of EXIT charts, designing a concatenated code is simplified to fit the curves of two decoders' EXIT functions [13, 15]. However, it is necessary to devise a way to measure the mutual information I_A and I_E of a decoder before we start to discuss the properties of EXIT charts. One way to measure the mutual information is presented by Hagenauer [15].

3.2.2 Properties of EXIT Charts

As presented by Brink, the information transfer function for iterative decoding and the process of iterative decoding can be visualized by the EXIT chart. In the concatenated code modeled in Fig.3.2 and for the first half of the iteration, the EXIT chart plots the mutual information generated by an inner decoder (space-time decoder) versus the mutual information coming from the outer decoder, which is modeled by the extrinsic channel in Fig.3.4 and the AWGN channel in Fig.A.1. In other words, the output of the lower branch in Fig.A.1 (I_A) determines the values of the horizontal axis of the EXIT chart and the output of the upper brunch in Fig.A.1 (I_E) determines the values of the vertical axis. Note that because these two quantities comprise the mutual information between binary data and its L-value, both range between zero and one. For the next half of the iteration, two decoders exchange their roles and hence the output of the inner decoder (space-time decoder) becomes the a priori input to the outer decoder. Notably unlike the inner decoder whose output depends on the information from the communication channel and the extrinsic channel, the outer code only takes the information from the extrinsic channel, which means that only the a priori information

will affect the output of the outer decoder. The separating property of iterative decoding allows us to observe and optimize the inner and outer codes separately.

Next we look at some examples in order to introduce how an EXIT chart works. Fig.3.5 is an EXIT chart for an inner decoder using a 16-QAM LD code as the inner code for a specific channel realization. As mentioned before, the inner decoder will receive information from the communication and extrinsic channels; therefore, even though there is no a priori information (I_A = 0) from the extrinsic channel or outer decoder, the inner decoder can still generate nonzero extrinsic information ($I_E \neq 0$) as shown in the figure. Note that, in this case, the EXIT transfer function $I_E = T_{in}(I_A)$ is an increasing function of I_A.

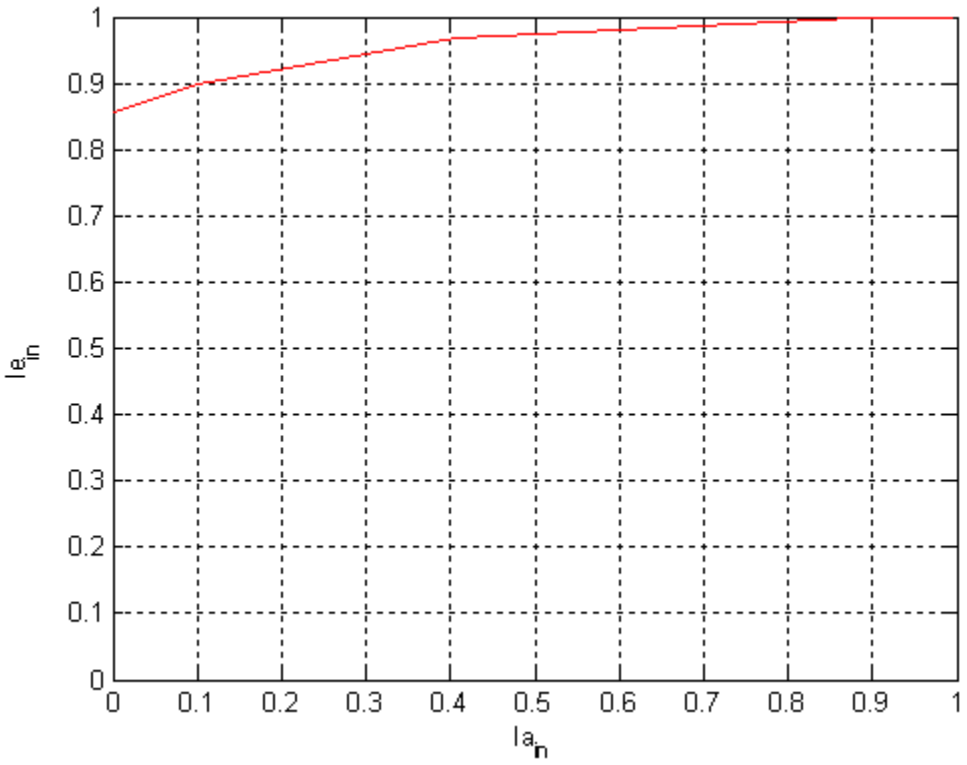

Fig.3.5 EXIT chart for a 16-QAM LD code at a channel realization $H = \begin{bmatrix} 1.6820 & 0.6122 \\ -0.0306 & 0.0841 \end{bmatrix}$ with SNR 19dB at each receive antenna

Fig.3.6 is an EXIT chart for a rate 0.9 LDPC code. This code will be concatenated with the 16-QAM LD code in Fig.3.5 as an outer code. Unlike the inner decoder, the EXIT function of the outer code only depends on the a priori information from the extrinsic channel or inner decoder and is not dependent on the channel parameters. Therefore, if the incoming a priori information I_A is zero, the outgoing extrinsic information I_E will be zero. Another observation form Fig.3.6 is that the extrinsic information generated by this decoder changes rapidly when the a priori information is greater than a threshold. This shows that this LDPC code will not be decoded with arbitrarily small error probability until the input a priori information is large enough.

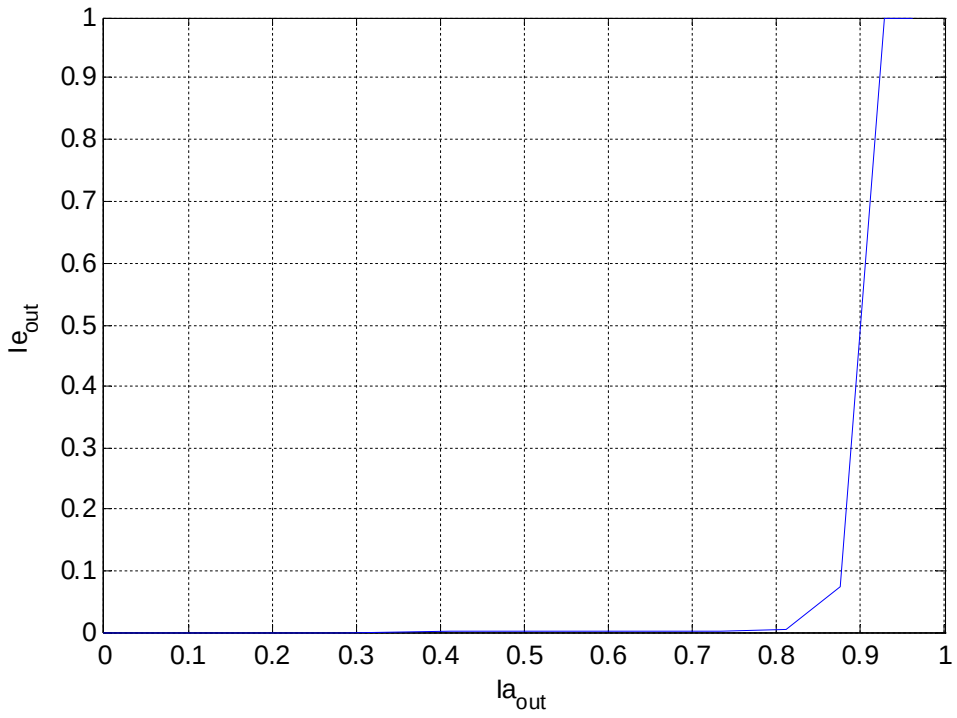

Fig.3.6 EXIT chart for an outer decoder (LDPC code with rate 0.9)

In a concatenated code, the iterative decoding process can be shown as Fig.3.3. During the first half of the iteration, the inner decoder will take the information from the channel and the outer decoder to generate extrinsic information which will be taken as a

priori information by the inner decoder at the next half of the iteration. This process can be visualized by an EXIT chart as shown in Fig.3.7.

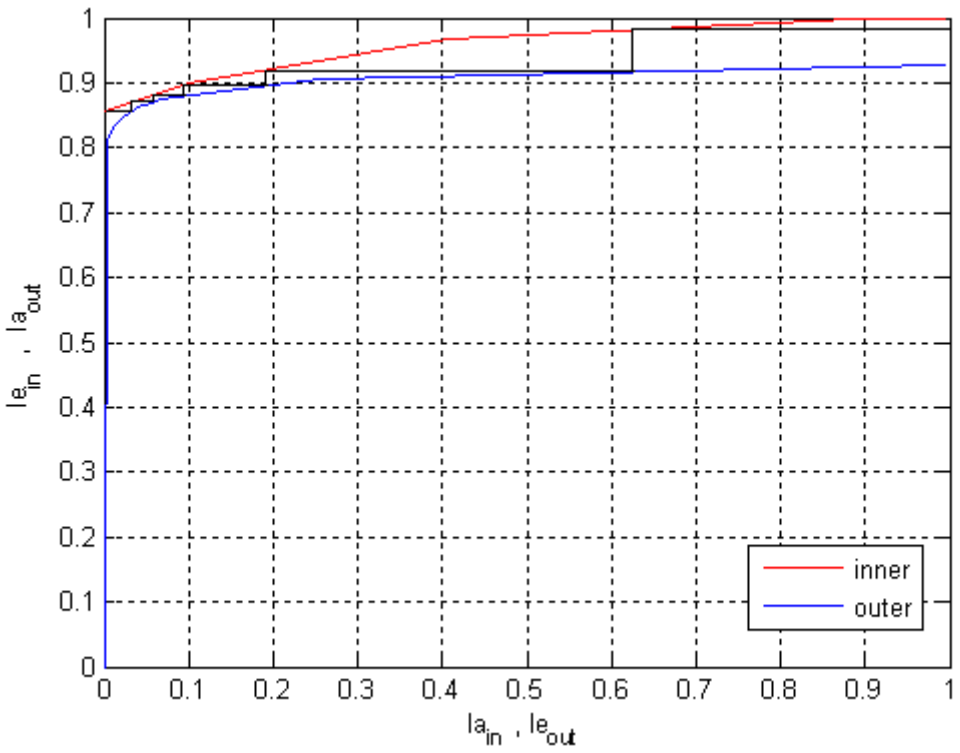

Fig.3.7 EXIT chart and the iterative decoding for a serial concatenated code with a 16-QAM LD code as the inner code and a rate 0.9 LDPC code as the outer code at a channel realization $H = \begin{bmatrix} 1.6820 & 0.6122 \\ -0.0306 & 0.0841 \end{bmatrix}$ with SNR 19dB at each receive antenna

Note that in Fig.3.7 the horizontal axis represents I_A for the inner decoder and I_E for the outer decoder while the vertical axis represents I_E for the inner decoder and I_A for the outer decoder. The mutual information being exchanged between inner and outer decoder can be tracked easily on an EXIT chart. The black line in Fig.3.7 shows how this mutual information evolves with the iteration. Eventually the mutual information passes the threshold of the outer code (LDPC code) and the serial concatenated code can

be decoded with arbitrarily small error probability at channel realization H= [1.6820 0.6122;-0.0306 0.0841] with SNR 19dB at each receive antenna.

However, the average mutual information in iterative decoding does not always converge to (1,1) in the EXIT chart. For example, Fig.3.8 is the EXIT chart for the serial concatenated code mentioned above at another channel realization. As shown in Fig.3.8, two EXIT function curves intersect at a point not equal to (1,1); thus this serial concatenated code cannot successfully be decoded at the channel realization H'= $\begin{bmatrix} 0.55 & 0 \\ 0 & 0.55 \end{bmatrix}$.

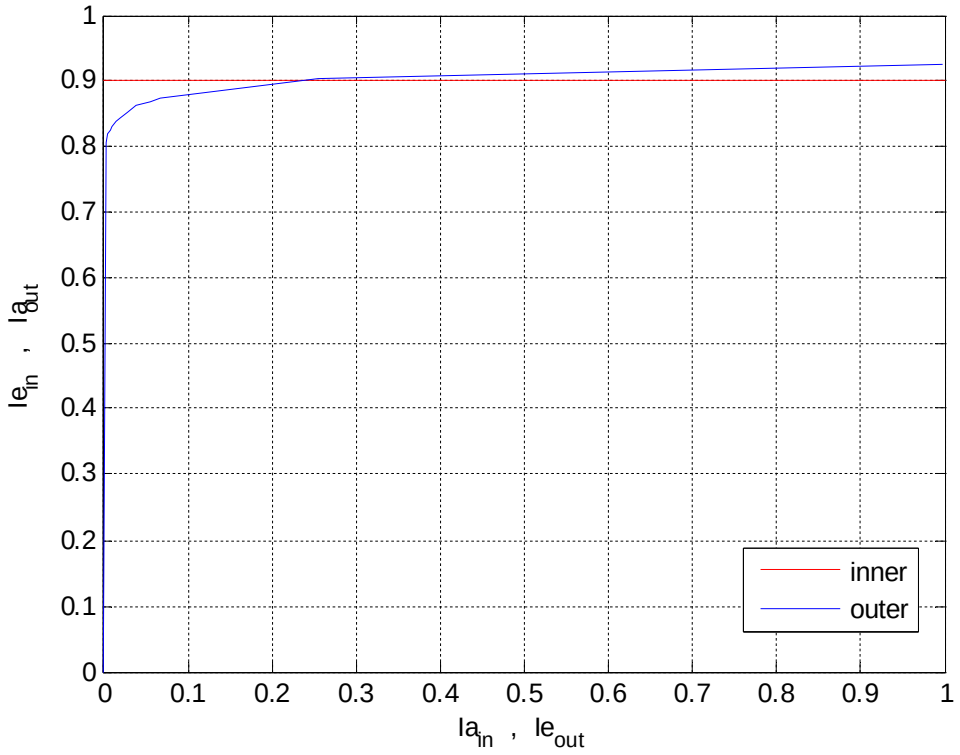

Fig.3.8 EXIT chart and the iterative decoding for a serial concatenated code with a 16-QAM LD code as the inner code and a rate 0.9 LDPC code as the outer code at a channel realization $H' = \begin{bmatrix} 0.55 & 0 \\ 0 & 0.55 \end{bmatrix}$ with SNR 19dB at each receive antenna

One important property of EXIT charts is called the area property which is proved in [12] when the extrinsic channel in Fig.3.4 is modeled as a binary erasure channel (BEC). For a serial concatenated coding scheme and channel state having the EXIT chart shown in Fig.3.7, the area property shows that

- For a rate R inner code, the area under the EXIT function curve is approximately equal to the capacity of the communication channel divided by the inner code rate R, that is

$$\int_0^1 T_{in}(I_A)dI_A \approx \frac{C_{comm.}}{R} = C_{bit}$$

- For a rate R_{out} outer code, the area on the left of the EXIT function curve is approximately equal to R_{out}, that is

$$\int_0^1 T_{out}^{-1}(I_E)dI_E \approx R_{out}$$

where C_{bit} is the communication channel capacity evaluated at the bit level. For the case in Fig.3.6, the channel capacity $C_{comm.}$ of H is approximately 7.8 bits/s/Hz and the inner code rate R is 8 bits per channel use, thus the capacity at the bit level C_{bit} is 0.97 which is the area under the EXIT curve of the inner code as shown in Fig.3.5. For the outer code case shown in Fig.3.6, the area on the left hand side of the EXIT curve is equal to the rate of the outer code. On the other hand, Fig.3.8 shows a channel realization H' with capacity 7.2 bits/s/Hz and the area under the EXIT curve of the inner code is 0.9, which is equal to the rate of the outer code. However, the iterative decoding cannot decode with arbitrarily small error probability because of the intersection of the two EXIT curves.

One can say that for a serial concatenated code if $R_{out} < C_{bit}$ and the two EXIT function curves do not intersect, the serial concatenated code can be decoded with arbitrarily small error probability by iterative decoding as shown in Fig.3.7. The area of the gap between two EXIT function curves can be viewed as the rate loss or sub-optimality of the coding scheme when used with an iterative decoder (see Fig.3.9).

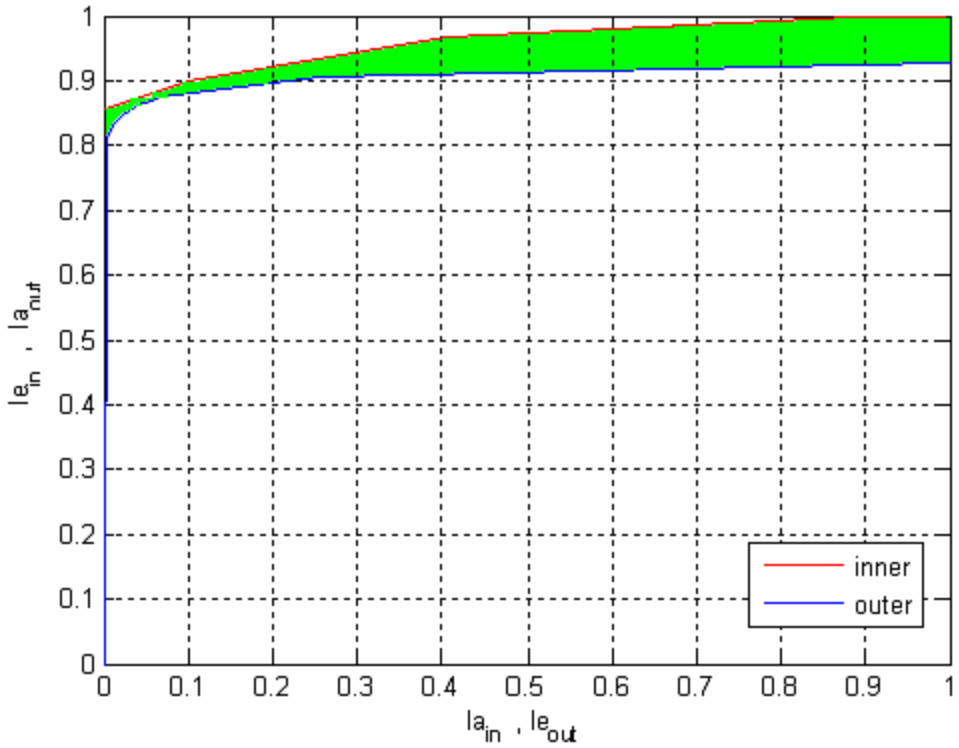

Fig.3.9 Rate lost of the serial concatenated code mentioned in Fig.3.7

where the green area between EXIT curves of the inner code and outer code represents the total rate loss of this serial concatenated code for the channel realization *H*. For most communication systems, transmitting at a high data rate is desired. From information theory, we know that the limit of data rate for successful transmission is the channel capacity. Therefore, we also want to design a serial concatenated code, such that the EXIT curves of the inner and outer codes are as close as possible in order to reduce the rate loss.

With the help of EXIT charts, designing a serial concatenated code involves fitting the EXIT curves of the inner and outer codes in a way such that the two curves are close but do not intersect. Therefore, we can design the LDPC code (outer code) to make the EXIT function of the iterative decoder fit the EXIT function curves of the space-time modulator (inner code). *However, the EXIT function of the inner code is a function of a*

priori information and the channel realization and signal-to-noise ratio, and the EXIT curves may change for different channel realizations. In order to design a robust serial concatenated code, it is necessary to study the EXIT functions of a space-time code for different channel realizations. In the next chapter, EXIT charts of VBLAST, LD codes and the Golden Code at different channel realizations with the same capacity are presented and a robust serial concatenated code is designed based on these results.

CHAPTER IV

DESIGN OF A CONCATENATED CODE FOR THE SLOW RAYLEIGH FADING CHANNEL

In this chapter, a robust serial concatenated code for the 2×2 slow Rayleigh fading channel will be designed. Our approach is to take the space-time code as a modulator and design an outer code such that the EXIT chart of the outer decoder does not intersect with the EXIT chart of the inner decoder for a set of channel realizations. We show how to choose this set of realizations and show that such a strategy results in good concatenated coding schemes.

Conventionally, there are two ways to design codes for non-binary modulation: multilevel coding and bit interleaved coded modulation. Both methods together with the technique of EXIT chart matching can produce an optimal concatenated space-time code that can have arbitrarily small error probability at the receiver for a fixed channel realization. However, for other channel realizations, such a code may fail to achieve arbitrarily small error probability at the receiver. It is difficult for us to design a fixed rate code by these two methods such that the system can still have arbitrarily small error probability for many different channel realizations. Therefore, to design a practical concatenated space-time code, we need an appropriate approach and criterion to evaluate the performance of the concatenated space-time code.

In this thesis, our approach to design a practical concatenated space-time code is designing a code that can achieve arbitrarily small error probability in a set of channels. This can be done by first drawing all EXIT curves of the space-time modulator in all channels in the set, and then designing an outer code whose EXIT curve matches the lower hull of all EXIT curves of the space-time modulator. In a slow fading channel, one can achieve arbitrarily small error probability at the receiver if the channel is not in outage; therefore, it is our goal to design a concatenated space-time code for a MIMO system that achieves arbitrarily small error probability when the channel is not in outage.

The outer code designed by this approach is suboptimal because its EXIT curve can not be matched to the EXIT curves of the space-time modulator for all the channel realizations which are not in outage. Thus, there will be rate-loss for this concatenated space-time code. The amount of rate loss depends on the “variation” of the EXIT charts of the space-time demodulator for this set of channels. Hence, we propose a design criterion: a good space-time code should stabilize its EXIT chart over different channel realizations, i.e., given a set of channel realizations, all of which have a capacity of R, the EXIT charts for the space-time demodulator for all the channels in this set should show very little variation. We refer to this as the space-time code stabilizing the channel and essentially presenting a single channel realization to the outer code. Note however, that we do not require for this equivalent channel to be memoryless.

In this chapter, we show that EXIT charts of the Golden Code have lesser variation over different channel realizations among all three space-time codes introduced in chapter II, and Golden Code can be used as the space-time modulator of a concatenated space-time code. We now discuss the design of concatenated code based on BICM as well as Multi-level coding.

4.1 Bit Interleaved Coded Modulation

For a system as shown in Fig.3.2, the space-time modulator and the outer code can be designed by matching their EXIT charts drawn at the demodulator and the decoder. For a fixed channel, to design a Concatenated space-time code by bit interleaved coded modulation (BICM), one can either choose a space-time modulator and design a outer code whose its EXIT chart matches the EXIT chart of the space-time demodulator, or choose an outer code and design a space-time modulator whose EXIT chart matches the EXIT chart of the outer code.

A concatenated space-time code design by BICM can be decoded with arbitrarily small error probability in a fixed channel, however, it may fail to be decoded with arbitrarily small error probability in another fixed channel. For example,

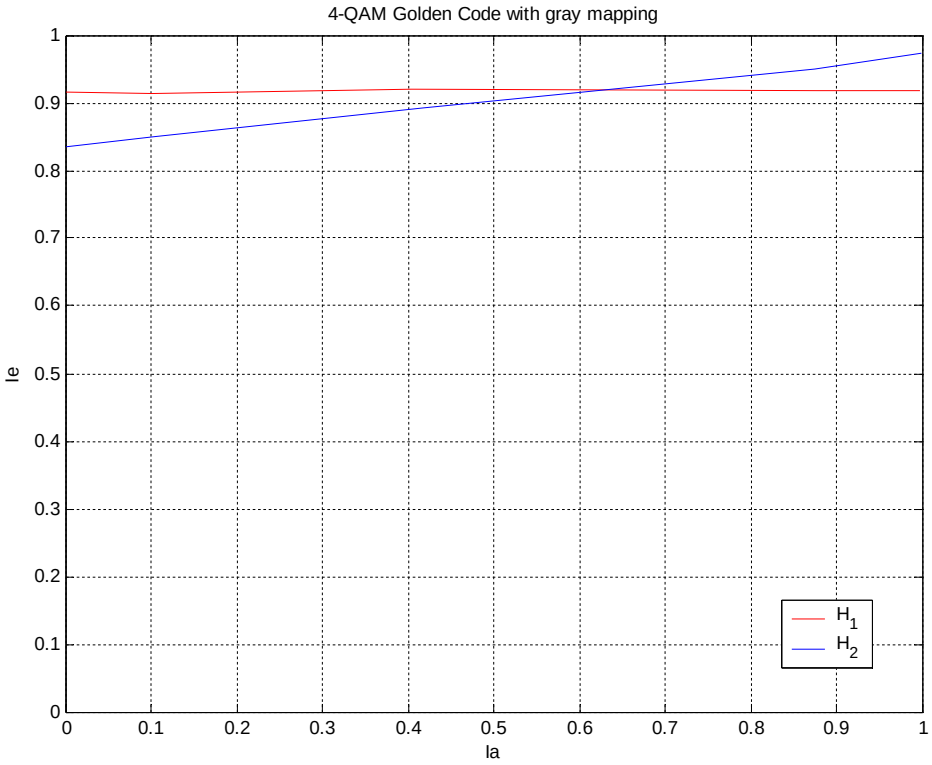

Fig.4.1 EXIT charts of 4QAM Golden Code with gray mapping in two different channels, H_1 = [0.55 0; 0 0.55] and H_2 = [1.17 0; 0 0.039], $C_{H1} = C_{H2}$ = 3.6 bits/s/Hz

Fig.4.1 shows two EXIT charts of a space-time demodulator received signal (we will call it ST EXIT charts in following contents) for two different channels. Clearly, these two charts are different even though the capacity of H_1 and H_2 are the same. Note that the area under the blue line and the red line in the figure are the same, but the shapes of the two curves are different. The optimal outer code for the space-time modulator in H_1

should have an EXIT chart matching the red line, but this optimal outer code for H_1 can not be decoded if the channel changes from H_1 to H_2.

4.2 Multilevel Coding

Another way to design a system shown in Fig.3.2 is to use multilevel coding (ML). It is an approach for constructing a high bandwidth efficiency coded modulation scheme. [19] considered multilevel codes as inner codes for a serial concatenation with an outer convolutional code. We can use this idea to design a multilevel LDPC code as the outer code for a serial concatenation with a space-time modulator as the inner code. First we take a look at the multilevel LDPC encoder.

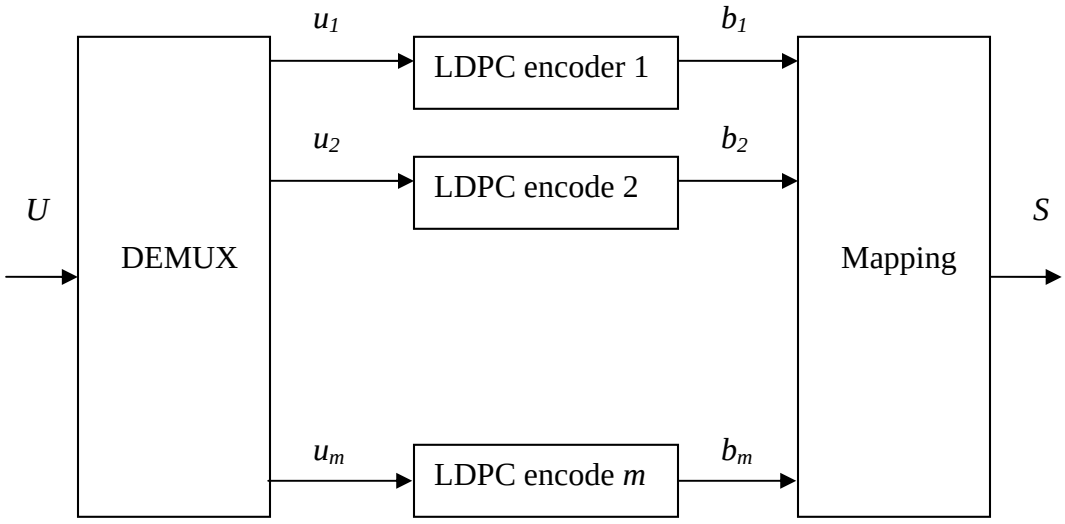

Fig.4.2 Multilevel LDPC encoder

where U is the binary information data string, u_i, $i = 1 \ldots m$ is the demultiplexed data string and b_i, $i = 1 \ldots m$ is the binary output of LDPC encoder i. m is the number of bits contained in a mapped symbol, for example, $m = 2$ if mapping is 4-QAM, and $m = 4$ if

mapping is 16-QAM. S is a one dimensional vector whose jth entry is a symbol mapped from binary vector [$b_1(j)$ $b_2(j)$… $b_m(j)$], and S will be encoded by the inner space-time code. With this technique, the ith bit in a mapped symbol can be encoded with the ith bits in other symbols. Therefore, we can design a specific LDPC code for all ith bits in mapped symbols. In order to do so, it is necessary to observe the EXIT chart of the ith bits in mapped symbols.

Since the elements of S are mapped from b_i, the length of b_i, $i = 1…m$ must be the same. On the other hand, LDPC encoder for ith level with rate R_i can be designed specifically for ith level and the length of u_i, $i = 1…m$ may be different from each other. The overall code rate of multilevel LDPC code shown in Fig.4.2 is the sum of [R_1 R_2 … R_m]. The outer code rate for each level can also be obtained by the chain rule of information according to:

$$I(b_1, b_2 ... b_m; Y) = I(b_1 \mid Y) + I(b_2 \mid b_1, Y) + ... + I(b_m \mid b_1 b_2 ... b_{m-1}, Y) \tag{4.1}$$

where the left hand side is the capacity of the channel, the first term of the right hand side is the outer code rate of the first level, the second term is the outer code rate of the second level and the mth term is the outer code rate of the mth level.

For decoding multilevel codes, the multistage decoder shown in Fig.4.3 can be used to decode each level code separately.

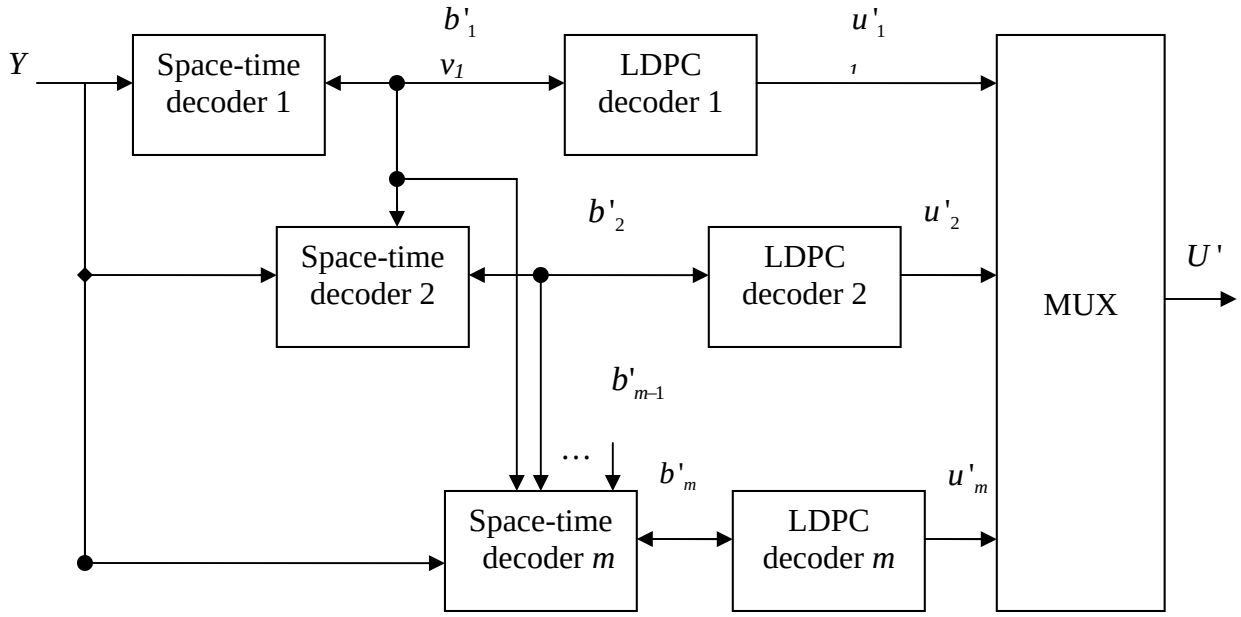

Fig.4.3 Multistage decoder

At stage *i*, the APP space-time decoder will receive signal *Y* from communication channel and $[b'_1\ b'_2\ ...\ b'_{i-1}]$ from previous *i*-1 stages as perfect a priori information. Iterative decoding is performed between APP decoder and LDPC decoder to generate the log likelihood ratio for b_i, and b'_i is its hard decision.

From the description of the multistage decoder, at each stage the space-time decoder only has partial information of the binary data. For instance, stage *i* only has information of $[b_1\ b_2\ \ldots\ b_i]$, whereas the space-time decoder in Fig.3.2 has information of $[b_1\ b_2\ \ldots\ b_m]$. Although the space-time decoders do not have full information except the decoder in last stage, the fact that the LDPC code is designed specifically for each stage allows each stage to have perfect knowledge of the data from previous stages, thus high rate LDPC codes can be used for higher stages. This may further reduce the rate loss of a serial concatenated code. On the other hand, if one of the stages provides incorrect information, the multistage decoder will fail to decode with arbitrarily small error probability.

The main problem in the design of multilevel codes for the slow Rayleigh fading channel is that the optimal rate of the LDPC codes to be used in the ith level depends on the channel realization, i.e. two different channel realizations can have the same I(X;b1b2..bm) whereas I(X;bi|b1,b2,..bi) can be different for the two realizations. Hence, it is not possible to pick the rates optimally for both realizations. Again, a good space-time code should stabilize the rates I(X;bi|b1,b2,..bi-1) for different channel realizations which have the same overall capacity.

4.3 An Appropriate Approach to Design a Practical Concatenated Space-time Code

From previous sections, we know that both BICM and ML can design a concatenated space-time code that only works in a specific fixed channel and is not practical. In order to design a practical concatenated space-time code that achieves arbitrarily small error probability in different channels, we need an appropriate design approach and criterion.

We can design an outer code that works in different channels with a given space-time modulator. For instance, an outer code can be designed for H_1 and H_2 in Fig.4.1, such an outer code has EXIT curve that matches the blue curve in Fig.4.1 when $0 \leqq I_a \leqq 0.6$ and matches the red curve when $0.6 \leqq I_a \leqq 1$. Together with the given space-time modulator, the system can have arbitrarily small error probability in H_1 and H_2. Notice that this is a suboptimal design approach because the system will always have a rate loss. The amount of the rate lost will depends on the "variation" of ST EXIT charts; therefore, our design criterion for Concatenated space-time code is that "a good space-time modulator should have less EXIT chart variation in different channels."

Now the problem is how to pick the set of channels so that we can draw EXIT functions of the space-time demodulator for these realizations. In next section, we will chose a transmission rate and draw a set of channel samples that can support this rate.

4.4 Channel Samples

In order to observe the variation of EXIT charts for space-time modulators, first we need to fix the transmission rate of the system and then draw channel samples that can support this rate, in other words, the system has to decode with arbitrarily small error probability in channels with a given channel capacity. Therefore, an approach to draw channel realizations from a given capacity is necessary. This can be done by using the 2×2 channel of the form in [17]

$$H = \begin{bmatrix} r\lambda & 0 \\ 0 & \lambda \end{bmatrix} \begin{bmatrix} \cos(\phi) & \sin(\phi)e^{j\theta} \\ -\sin(\phi) & \cos(\phi)e^{j\theta} \end{bmatrix} \tag{4.2}$$

where $r \geqq 1$ is the ratio between two eigenvalues of H, $\lambda \geqq 0$ is the smaller eigenvalue of H, and $\phi \in [0, 2\pi)$, $\theta \in [0, 2\pi)$.

Insert (4.2) into (2.5), for a given capacity, the values of ϕ and θ do not change the given capacity since the second matrix in (4.2) is an unitary matrix, therefore the capacity of (4.2) can be written as

$$\begin{aligned} C &= \log_2 \det\left(\begin{bmatrix} 1 & 0 \\ 0 & 1 \end{bmatrix} + \frac{\rho}{2} \begin{bmatrix} r\lambda & 0 \\ 0 & \lambda \end{bmatrix} \begin{bmatrix} r\lambda & 0 \\ 0 & \lambda \end{bmatrix} \right) \\ &= \log_2 \left(1 + \frac{\rho}{2}(r\lambda)^2\right)\left(1 + \frac{\rho}{2}\lambda^2\right) \end{aligned} \tag{4.3}$$

where ρ is the received SNR at each receive antenna. From (4.3), a channel with given capacity can be sampled either by the variable r or λ.

Before the range of r being defined, we should first set a given capacity C and the received SNR ρ at each antenna. As mentioned before, we would like to design a high rate code which can decode successfully in every channel whose capacity is lager than the rate of the code. Recall that the rate of the three space-time codes introduced in chapter II is $2\log_2 M$ if M-QAM is used. For the case of a space-time code with 4-QAM constellation being used as an inner code, the best rate can be achieved is 4 bits/s/Hz, thus by information theory, an ideal space-time code with 4-QAM constellation should

be able to communicate successfully at channel realizations with capacity $C>4$ bits/s/Hz. Therefore, for space-time codes with 4-QAM constellation, we fix the channel capacity at 3.6 bit/s/Hz and obtain a set of channels by changing r, ϕ and θ. EXIT charts for space-time codes at this set of channel samples can be drawn so that we can observe the EXIT charts variation of space-time codes. For the case of space-time codes with 16-QAM constellation, we fix the capacity at 7.4 bits/s/Hz.

Now we fix the capacity for a given space-time code, thus channel samples of this capacity can be drawn with different values of r, ϕ and θ. However, only the lower bound of r is defined ($r \geqq 1$) and the upper bound is needed to be set so that we can draw the channel samples by sampling r between the lower bound and the upper bound. We can apply the typical outage cases mentioned in [18] to set the upper bound of r for both 4-QAM and 16-QAM cases.

At high SNR ρ, it is shown in [18] that the typical way for outage to occur is when the largest k eigenvalues of a channel realization H are of order 1, while the rest are of the order $1/\rho$ or smaller; geometrically, H is close to a rank k matrix. For a channel model like (3.1), the outage occurs when $r \geqq \rho$ and H will close to a rank one matrix. With this result, the upper bound of r can be set as ρ and the range of channel eigenvalues ratio is $1 \leqq r \leqq \rho$.

For space-time codes with 4-QAM constellation, we set the received SNR ρ equivalent to 12 dB and the range of channel eigenvalues ratio r will be $1 \leqq r \leqq 20$. Similarly, the received SNR ρ is 19dB and the range of channel eigenvalues ratio r will be $1 \leqq r \leqq 80$

4.5 EXIT Charts of Space-time Codes

In this section, we will present EXIT charts of space-time codes (VBLAST, LD-STBC and Golden Code) for different channel realizations with the same capacity obtaining as explained in the previous section. We will first look at the case of VBLAST with 4-QAM constellation at capacity equal to 3.6 bits/s/Hz and discover some properties of this case.

4.5.1 EXIT Charts of Space-time Codes with 4-QAM Constellation

First, we discovered that for a fixed channel eigenvalue ratio r and received SNR ρ, the EXIT charts will depends on ϕ and θ in (3.1) but the area between the highest curve and the lowest curve will only depend on $\phi \in [0, \pi/2)$. An example for this property can be shown in the following figures where the variable for both cases is $\phi \in [0, \pi/2)$.

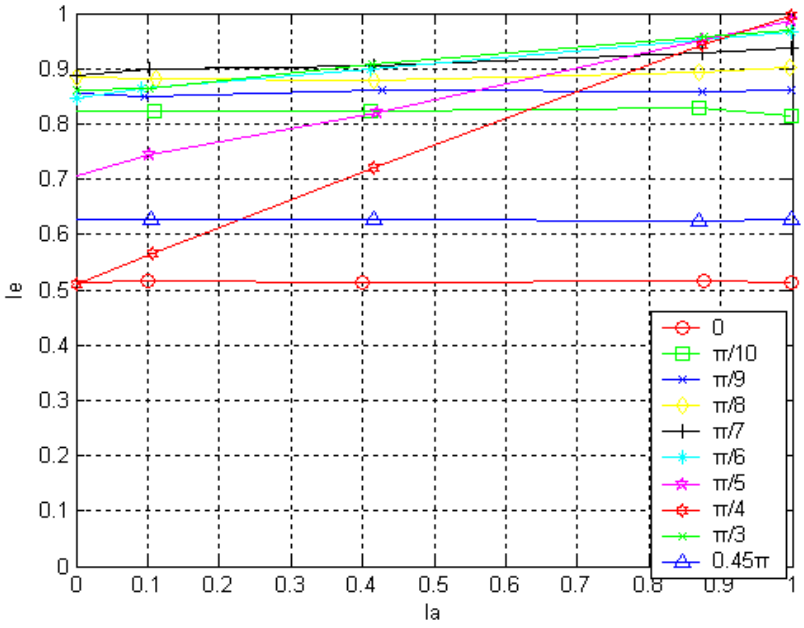

Fig.4.4 EXIT chart of 4-QAM VBLAST, C=3.6 bits/s/Hz, ρ=12dB, r =20, θ= 0

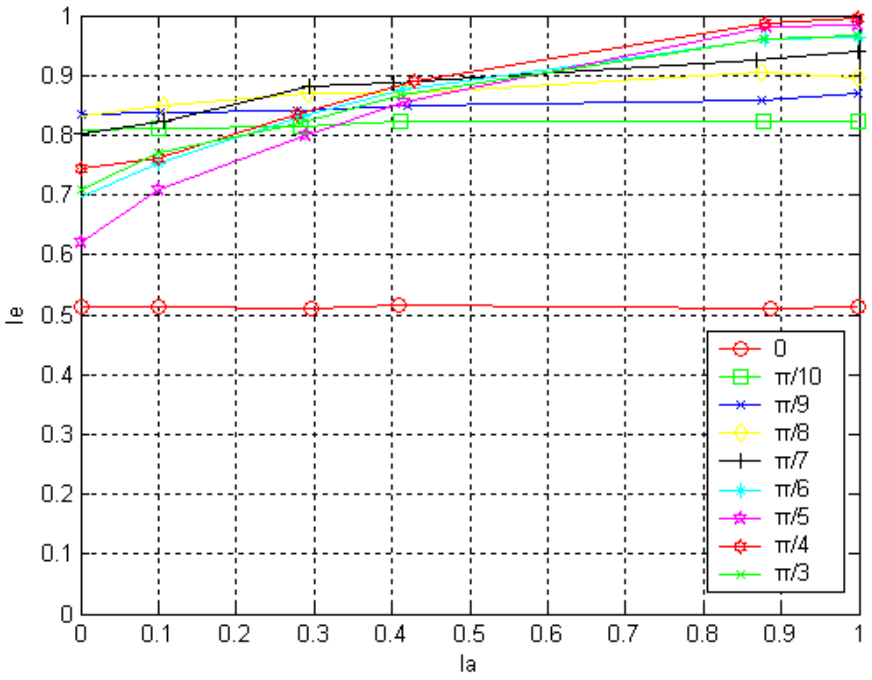

Fig.4.5 EXIT chart of 4-QAM VBLAST, C=3.6 bits/s/Hz, ρ=12dB, r =20, $\theta = \frac{\pi}{4}$

As shown in the figures, although the EXIT curves of these two charts are not exactly the same, the lowest curves of both EXIT charts are drawn when ϕ = 0 and are identical, also, the area between the highest curves and the lowest curves in these two charts are approximately the same. The reason that the area between the highest curves and the lowest curves mentioned here is because this area will determine the rate loss of a concatenated space-time code over a set of channel realizations with fixed capacity. For convenience, we call this area "the variation of EXIT curves".

For the cases of Fig.4.4 and Fig.4.5, if we want to design a concatenated space-time code with VBLAST as the space-time modulator, an outer code has to be designed in a way such that its EXIT curve matches the lowest EXIT curves in both figures. Such design will cost huge rate loss (approximately 0.4) for both cases. Hence, for VBLAST cases, it is enough to ignore the EXIT curves drawn with different θ since the rate lost is determined by the variation of EXIT curves.

Another factor to determine the variation of EXIT curves is the eigenvalue ratio of the channel. It will be shown that the variation will increase as the eigenvalue ratio increases until it reaches some threshold.

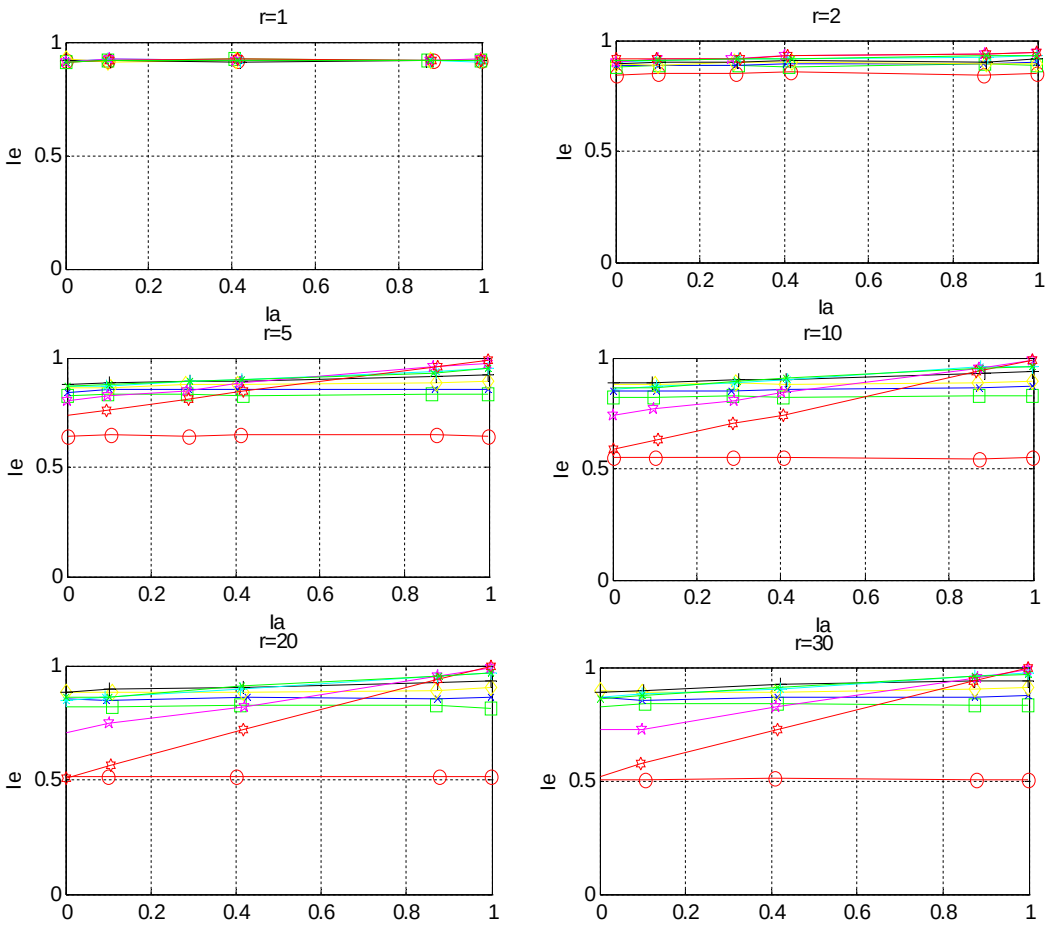

Fig.4.6 EXIT charts of 4-QAM VBLAST, C=3.6 bits/s/Hz, ρ=12dB, r = [1, 2, 5, 10, 20, 30], θ= 0

Fig.4.6 shows EXIT charts of 4-QAM VBLAST at channel capacity C=3.6 bits/s/Hz, received SNR ρ=12dB and eigenvalue ratio r = [1, 2, 5, 10, 20, 30]. Note that the EXIT chart for r = 20 is approximately identical to the EXIT chart for r = 30 because

both are typical outage cases as mentioned in the previous section. The variable for each chart in Fig.4.4 is ϕ and we found that the lowest curve for each chart is drawn when ϕ = [0, π/2, π, 3π/2], whereas EXIT curves for $\phi \in [0, 2\pi)$ and $\phi \neq$ [0, π/2, π, 3π/2] will be placed between the lowest curve and I_e = 1. Hence, It is sufficient to sample ϕ between 0 and π/2.

For the sake of convenience, all EXIT curves of the six charts in Fig.4.6 will be drawn in one chart as shown in Fig.4.7, so it will be easier to observe the variation of EXIT curves and we will continue to do so for other space-time codes.

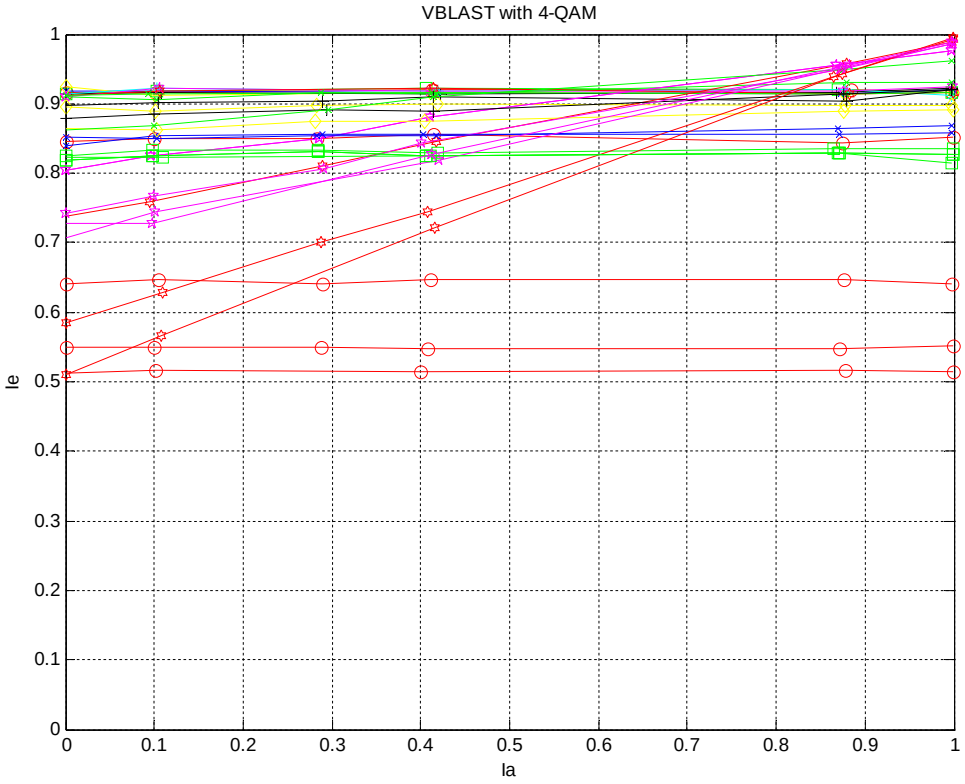

Fig.4.7 EXIT charts of 4-QAM VBLAST, *C*=3.6 bits/s/Hz, ρ=12dB, *r* = [1, 2, 5, 10, 20, 30], $\phi = [0, \frac{\pi}{10}, \frac{\pi}{9}, \frac{\pi}{8}, \frac{\pi}{7}, \frac{\pi}{6}, \frac{\pi}{5}, \frac{\pi}{4}, \frac{\pi}{3}]$, θ= 0

From Fig.4.7, if 4-QAM VBLAST is used as the space-time modulator of a system shown as Fig.3.2 which small error probability when the channel capacity $C \geqq 3.6$ bits/s/Hz, the outer code must be designed in a way such that its EXIT curve fits the lowest curve in Fig.4.7 and will have a rate lost about 0.4 bits/s/Hz at the bit level. This rate lost comes from the huge variation of the EXIT curves, especially when ϕ is zero or close to $\pi/2$ (ex: 0.45π, shown in Fig.4.4). The intuitive explanation for this result is the fact that the VBLAST does not code over time. A channel realization as (4.2) times a 4-QAM VBLAST codeword is the following:

$$\begin{bmatrix} r\lambda & 0 \\ 0 & \lambda \end{bmatrix} \begin{bmatrix} \cos(\phi) & \sin(\phi)e^{j\theta} \\ -\sin(\phi) & \cos(\phi)e^{j\theta} \end{bmatrix} \begin{bmatrix} a \\ b \end{bmatrix}$$
$$= \begin{bmatrix} r\lambda(a\cos(\phi) + b\sin(\phi)e^{j\theta}) \\ \lambda(-a\sin(\phi) + b\cos(\phi)e^{j\theta}) \end{bmatrix} \tag{4.4}$$

where *a* and *b* can be any symbol chosen from 4-QAM constellation. In (4.4), if ϕ is zero or close to $\pi/2$, the signal strength of *a* and *b* at the receiver will depend on *r* or λ. For a fixed capacity channel and ϕ is zero or close to $\pi/2$, if $r \neq 1$, the signal strength of *a* and *b* at the receiver will be different, and if r is large, one of the signal strength will become too small to be decoded. This property may cause VBLAST in outage at some channel samples and result in the large variation of EXIT charts for 4-QAM VBLAST and the requirement for a low rate outer code. This will lead to a rate loss of about 0.4 bits/s/Hz at the bit level if 4-QAM VBLAST is used as the space-time modulator of a system shown in Fig.3.2. According to this result, we can say that the 4-QAM VBLAST is not robust in 2×2 slow Rayleigh fading channel and is not a good space-time modulator for a robust concatenated space-time code.

It is shown in [15] that if the mapping of the QAM is selected in a proper way the a priori information of the other bits can improve the detection of the current bit even if the information from communication channel is remained the same. The previous EXIT charts are drawn from 4-QAM VBLAST with gray mapping and do not have any gain with increasing a priori information at some channel samples. EXIT curves drawn at

these channel samples are parallel to I_a axis and the iterative decoding will not improve the extrinsic information at these channel samples. Now we change the constellation from gray mapping to natural mapping as shown in Fig.4.8 and can see the variation of EXIT curves as shown in Fig.4.9.

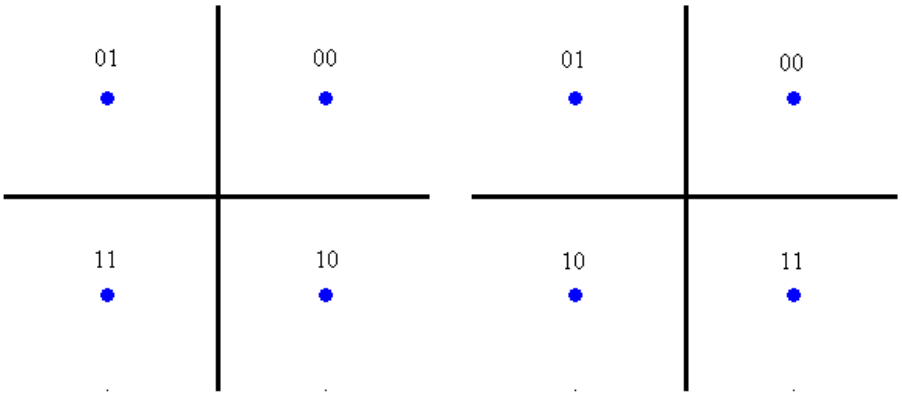

Fig.4.8 Gray mapping (left) and natural mapping (right) for 4-QAM

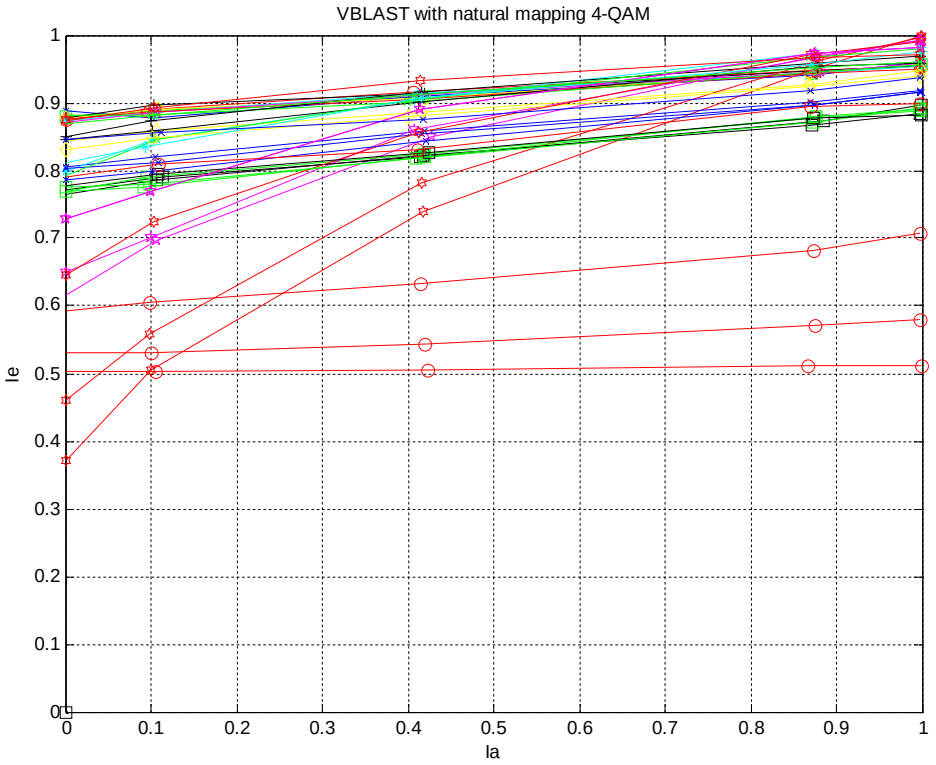

Fig.4.9 EXIT charts of VBLAST with natural mapping 4-QAM, C=3.6 bits/s/Hz, ρ=12dB, r = [1, 2, 5, 10, 20, 30], $\phi = [0, \frac{\pi}{10}, \frac{\pi}{9}, \frac{\pi}{8}, \frac{\pi}{7}, \frac{\pi}{6}, \frac{\pi}{5}, \frac{\pi}{4}, \frac{\pi}{3}]$, θ= 0

As shown in the Fig.4.9, most EXIT curves of VBLAST with natural mapping 4-QAM are not parallel to I_a axis and therefore the extrinsic information will increase with increase in the a priori information. Although the iterative decoding becomes helpful with natural mapping, the large variation of EXIT curves still brings large rate loss which is about 0.4 and does not change the fact that VBLAST is not robust in 2×2 slow Rayleigh fading channel.

Unlike VBLAST, the LD codes and Golden Code are space-time codes which encode information symbols over both antennas and time. For these two space-time codes, every information symbol is transmitted by two transmit antennas to receiver and is not lost if the eigenvalue λ in (4.2) is small. We can expect that the variation of EXIT

curves for these two space-time codes to be not as large as VBLAST. The followings are EXIT charts of 4-QAM LD code and 4-QAM Golden Code with different mappings. The channel capacity is 3.6 bits/s/Hz and the received SNR at each antenna is 12dB.

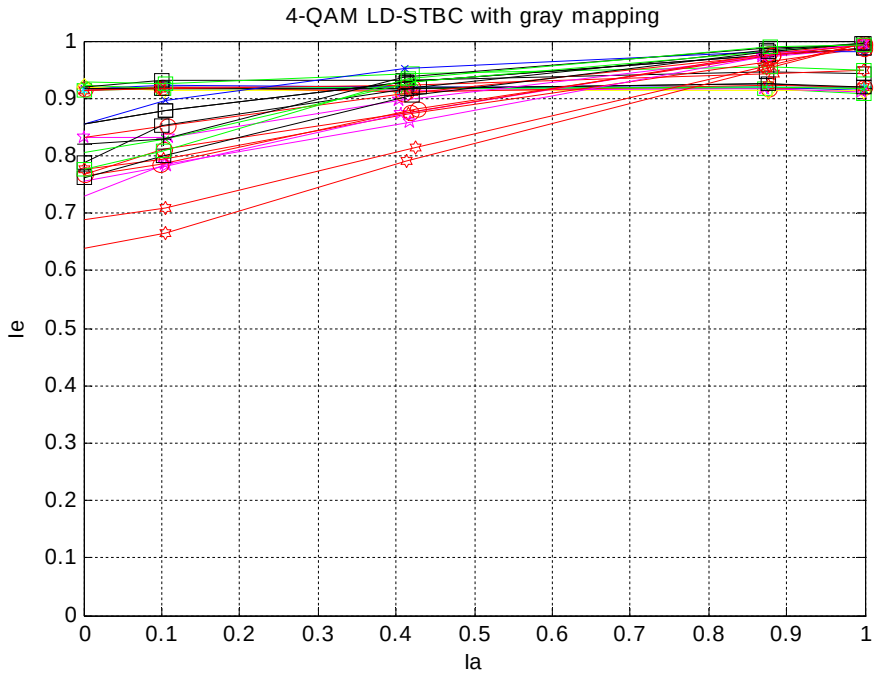

Fig.4.10 EXIT charts of LD code with gray mapping 4-QAM, C=3.6 bits/s/Hz, ρ=12dB, r = [1, 2, 5, 10, 20], $\phi = [0, \frac{\pi}{10}, \frac{\pi}{9}, \frac{\pi}{8}, \frac{\pi}{7}, \frac{\pi}{6}, \frac{\pi}{5}, \frac{\pi}{4}, \frac{\pi}{3}]$, θ= 0

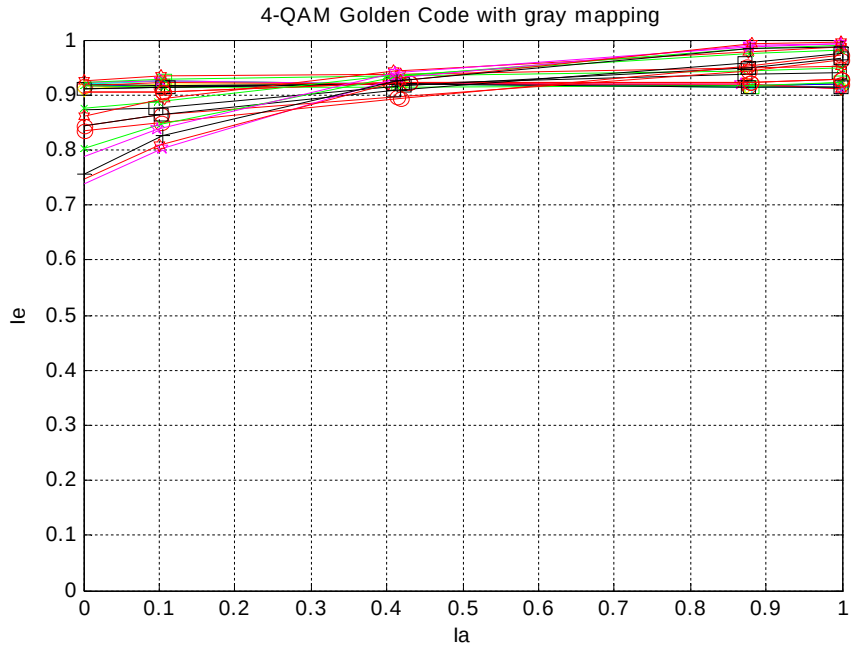

Fig.4.11 EXIT charts of Golden Code with gray mapping 4-QAM, C=3.6 bits/s/Hz, ρ=12dB, r = [1, 2, 5, 10, 20], $\phi = [0, \frac{\pi}{10}, \frac{\pi}{9}, \frac{\pi}{8}, \frac{\pi}{7}, \frac{\pi}{6}, \frac{\pi}{5}, \frac{\pi}{4}, \frac{\pi}{3}]$, θ= 0

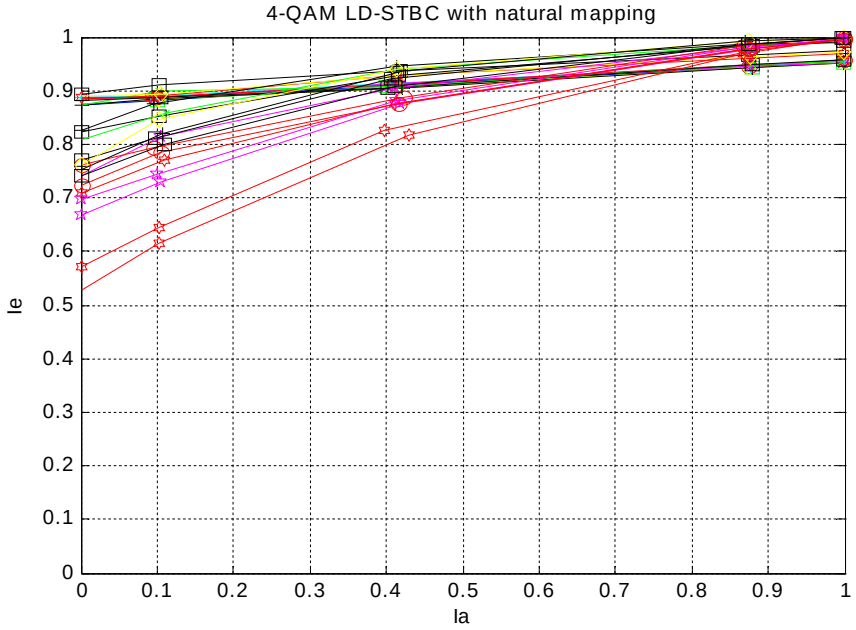

Fig.4.12 EXIT charts of LD code with natural mapping 4-QAM, C=3.6 bits/s/Hz, ρ=12dB, r = [1, 2, 5, 10, 20], $\phi = [0, \frac{\pi}{10}, \frac{\pi}{9}, \frac{\pi}{8}, \frac{\pi}{7}, \frac{\pi}{6}, \frac{\pi}{5}, \frac{\pi}{4}, \frac{\pi}{3}]$, θ= 0

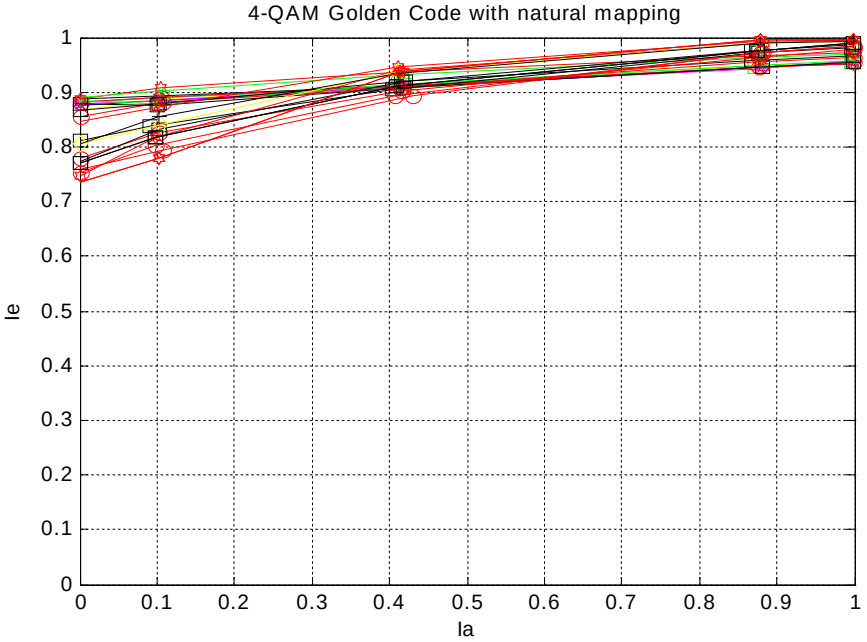

Fig.4.13 EXIT charts of Golden Code with natural mapping 4-QAM, C=3.6 bits/s/Hz, ρ=12dB, r = [1, 2, 5, 10, 20], $\phi = [0, \frac{\pi}{10}, \frac{\pi}{9}, \frac{\pi}{8}, \frac{\pi}{7}, \frac{\pi}{6}, \frac{\pi}{5}, \frac{\pi}{4}, \frac{\pi}{3}]$, θ= 0

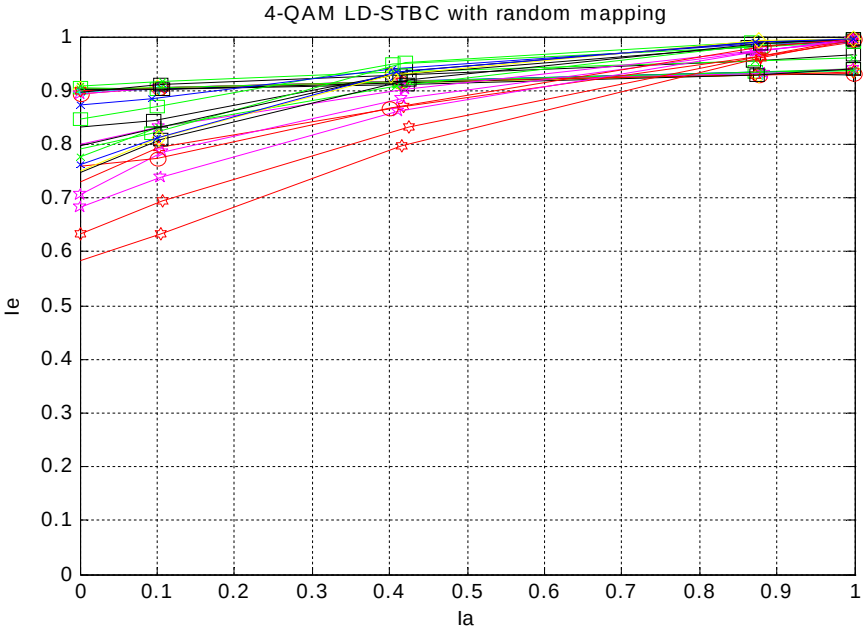

Fig.4.14 EXIT charts of LD code with random mapping 4-QAM, C=3.6 bits/s/Hz, ρ=12dB, r = [1, 2, 5, 10, 20], $\phi = [0, \frac{\pi}{10}, \frac{\pi}{9}, \frac{\pi}{8}, \frac{\pi}{7}, \frac{\pi}{6}, \frac{\pi}{5}, \frac{\pi}{4}, \frac{\pi}{3}]$, θ= 0

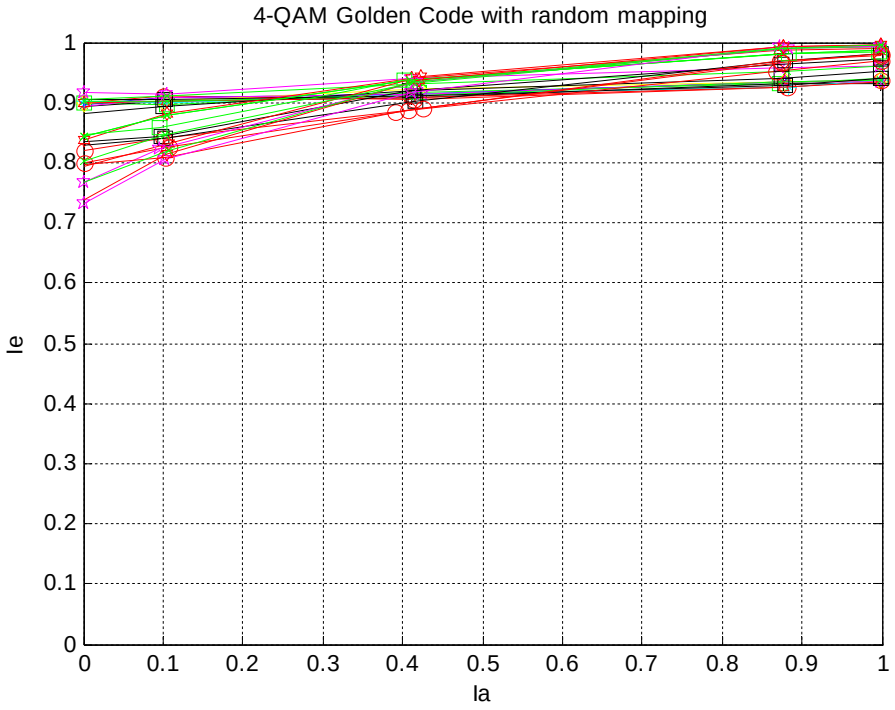

Fig.4.15 EXIT charts of Golden Code with random mapping 4-QAM, C=3.6 bits/s/Hz, ρ=12dB, r = [1, 2, 5, 10, 20], $\phi = [0, \frac{\pi}{10}, \frac{\pi}{9}, \frac{\pi}{8}, \frac{\pi}{7}, \frac{\pi}{6}, \frac{\pi}{5}, \frac{\pi}{4}, \frac{\pi}{3}]$, θ= 0

We can observe that for a specific space-time modulation, its EXIT charts are varying between different channel samples. We can also observe that all EXIT charts of Golden Code and LD code (Fig.4.10~Fig.4.15) show less variation compared with VBLAST. However, for some channel realizations, the EXIT curves of LD code have low extrinsic information at zero a priori information, for instance when r = [10, 20] and $\phi = \pi / 4$. The bad performance at these channel samples causes EXIT charts of LD code to have larger variation than Golden Code. For Golden Code, the area under the EXIT curves is about 0.86 regardless the mapping and therefore, an LDPC code can be used as the outer code with rate 0.86 at most. Similarly, the LD code can only be concatenated with an LDPC code with rate 0.8 at most and will cost more rate loss than Golden Code.

An explanation is stated in [6] that, for the 4-QAM Golden Code, the constellation of its codewords is almost a rotated regularly spaced QAM constellation with 16 distinct

points with same average energy as 4-QAM, whereas it is the union of PSK constellations for the 4-QAM LD code. The property of the codewords constellation along with the minimum value of δ_{min} are the key facto to explain why the performance of Golden Code is superior to LD code when a priori information is zero.

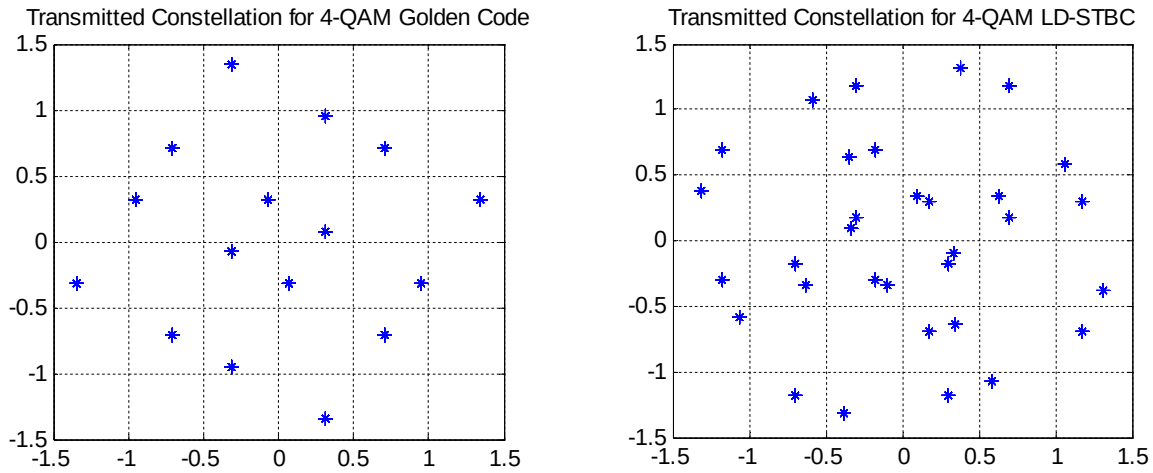

Fig.4.16 Transmitted constellation for 4-QAM Golden Code and LD code

4.5.2 EXIT Charts of Space-time Codes with 16-QAM Constellation

In this section, EXIT charts are drawn from 16-QAM space-time codes at 2×2 slow Rayleigh fading channel where capacity C is 7.4 bits/s/Hz and received SNR ρ is 19dB. The channel samples are obtained from (4.1) with $1 \leqq r \leqq 80$, $\phi \in [0, 2\pi)$ and $\theta \in [0, 2\pi)$. Again, the value of θ does not change the variation of EXIT curves and can be fixed at zero for convenience. Another observation is that the variation of a ST EXIT chart remains the same from $1 \leqq r \leqq 30$ to $1 \leqq r \leqq 80$, and therefore, it is enough to set

the upper bound of r at 30. We will also use three different mappings for 16-QAM and observe the variation of EXIT curves for different mapping.

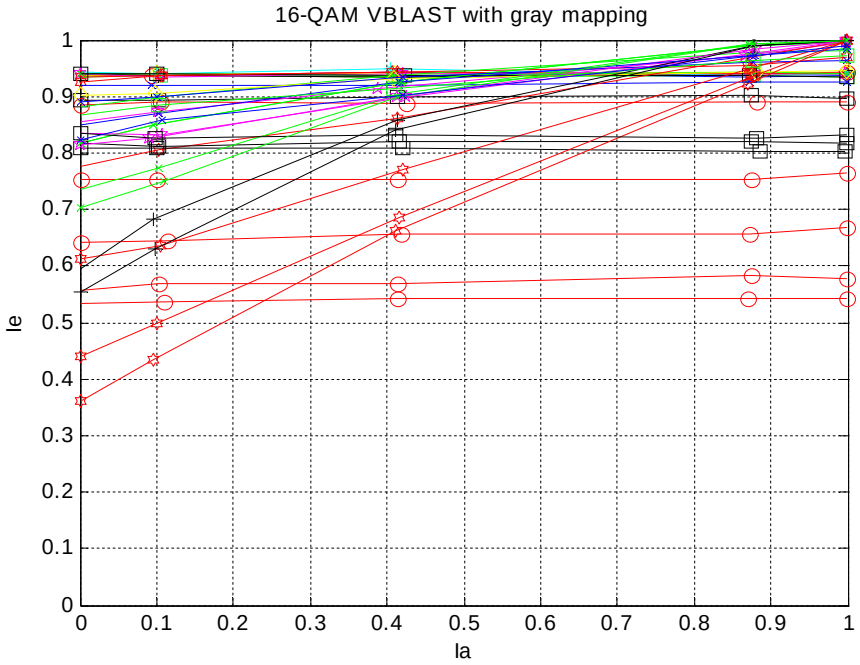

Fig.4.17 EXIT charts of VBLAST with gray mapping 16-QAM, C = 7.4 bits/s/Hz, ρ=19dB, r = [1, 2, 5, 10, 20, 30], $\phi = [0, \frac{\pi}{10}, \frac{\pi}{9}, \frac{\pi}{8}, \frac{\pi}{7}, \frac{\pi}{6}, \frac{\pi}{5}, \frac{\pi}{4}, \frac{\pi}{3}]$, θ= 0

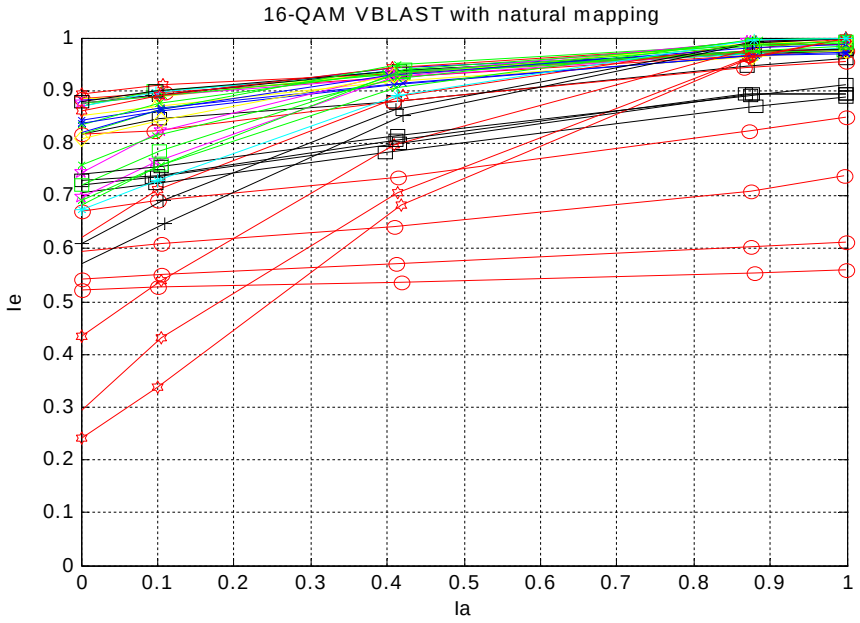

Fig.4.18 EXIT charts of VBLAST with natural mapping 16-QAM, C = 7.4 bits/s/Hz, ρ=19dB, r = [1, 2, 5, 10, 20, 30], $\phi = [0, \frac{\pi}{10}, \frac{\pi}{9}, \frac{\pi}{8}, \frac{\pi}{7}, \frac{\pi}{6}, \frac{\pi}{5}, \frac{\pi}{4}, \frac{\pi}{3}]$, θ= 0

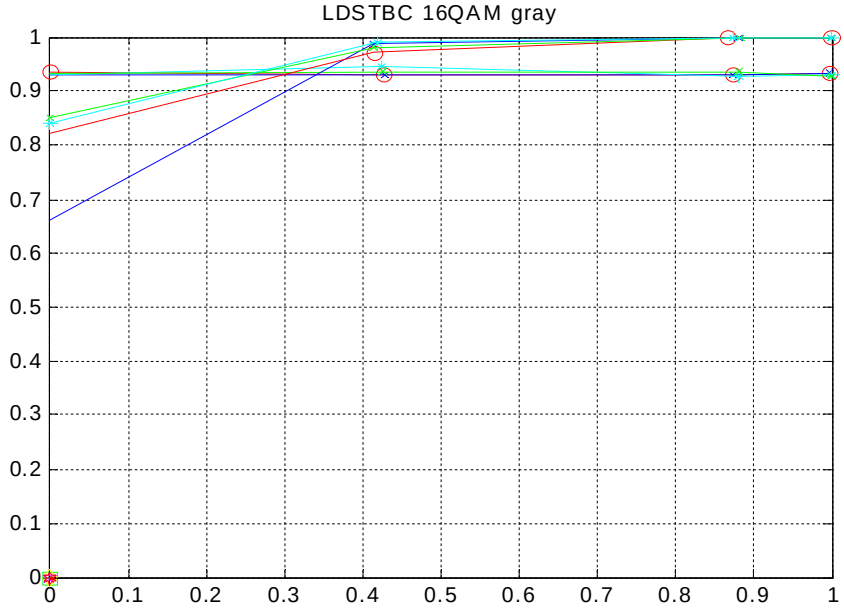

Fig.4.19 EXIT charts of LD code with gray mapping 16-QAM, C = 7.4 bits/s/Hz, ρ=19dB, r = [1, 2, 5, 10, 20, 30], $\phi = [0, \frac{\pi}{9}, \frac{\pi}{6}, \frac{\pi}{3}]$, θ= 0

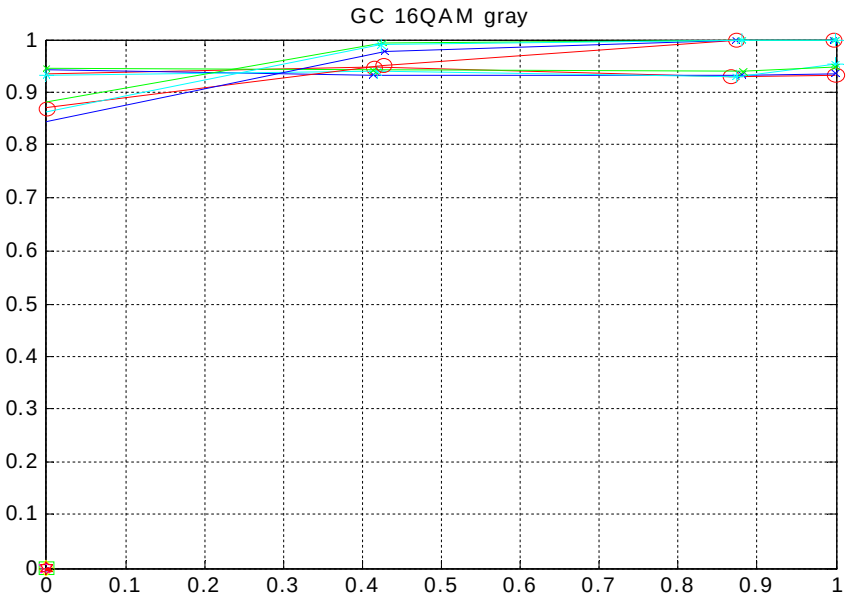

Fig.4.20 EXIT charts of Golden Code with gray mapping 16-QAM, C = 7.4 bits/s/Hz, ρ=19dB, r = [1, 2, 5, 10, 20, 30], $\phi = [0, \frac{\pi}{9}, \frac{\pi}{6}, \frac{\pi}{3}]$, θ= 0

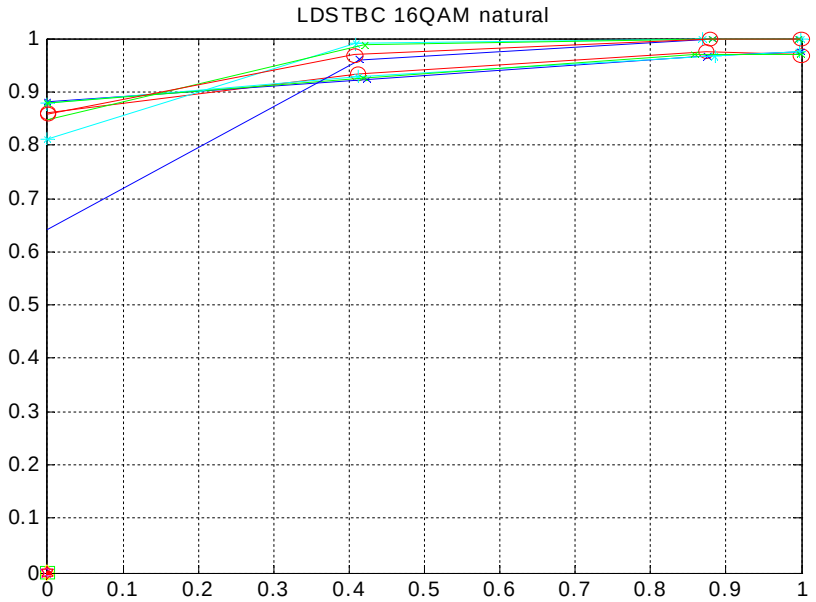

Fig.4.21 EXIT charts of LD code with natural mapping 16-QAM, C = 7.4 bits/s/Hz, ρ=19dB, r = [1, 2, 5, 10, 20, 30], $\phi = [0, \frac{\pi}{9}, \frac{\pi}{6}, \frac{\pi}{3}]$, θ= 0

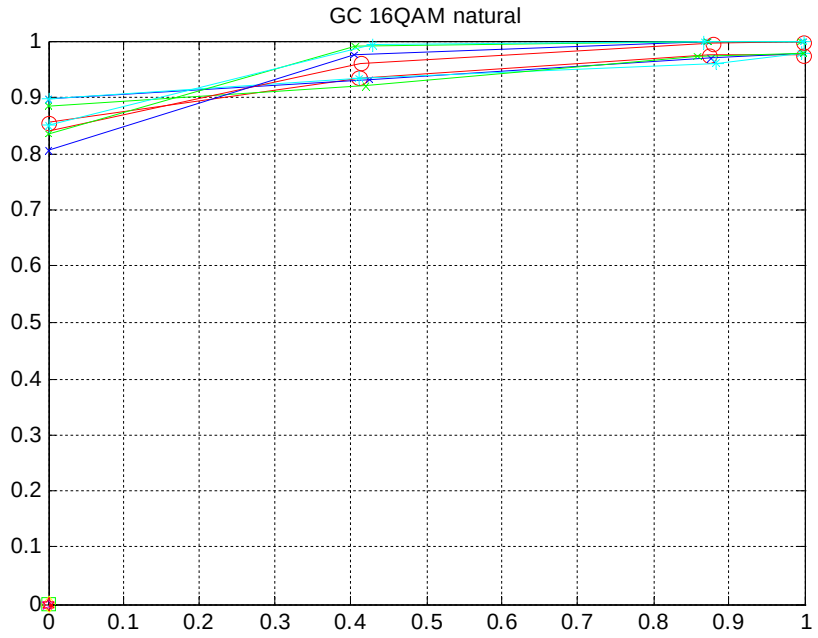

Fig.4.22 EXIT charts of Golden Code with natural mapping 16-QAM, C = 7.4 bits/s/Hz, ρ=19dB, r = [1, 2, 5, 10, 20, 30], $\phi = [0, \frac{\pi}{9}, \frac{\pi}{6}, \frac{\pi}{3}]$, θ= 0

It is clear that Golden Code results in the least variation in the EXIT curves among three space-time codes with 16-QAM constellation. The Golden Code can be concatenated with an LDPC code with rate 0.91 whereas the LD-STBC can only be concatenated with an LDPC code with rate 0.88. This will cost more rate loss than the 4-QAM LD-STBC.

4.6 The Design of Concatenated Space-time Codes with Multilevel Coding

Now we apply the multilevel coding technique to the system shown in Fig.3.2 where the Golden Code is used as space-time modulator to modulate *S*. First we take a look at the case when the bits to 4-QAM mapping is random and the space-time code is a Golden Code which makes *m*=2 in Fig.4.2 and Fig.4.3. The EXIT charts are shown as the following:

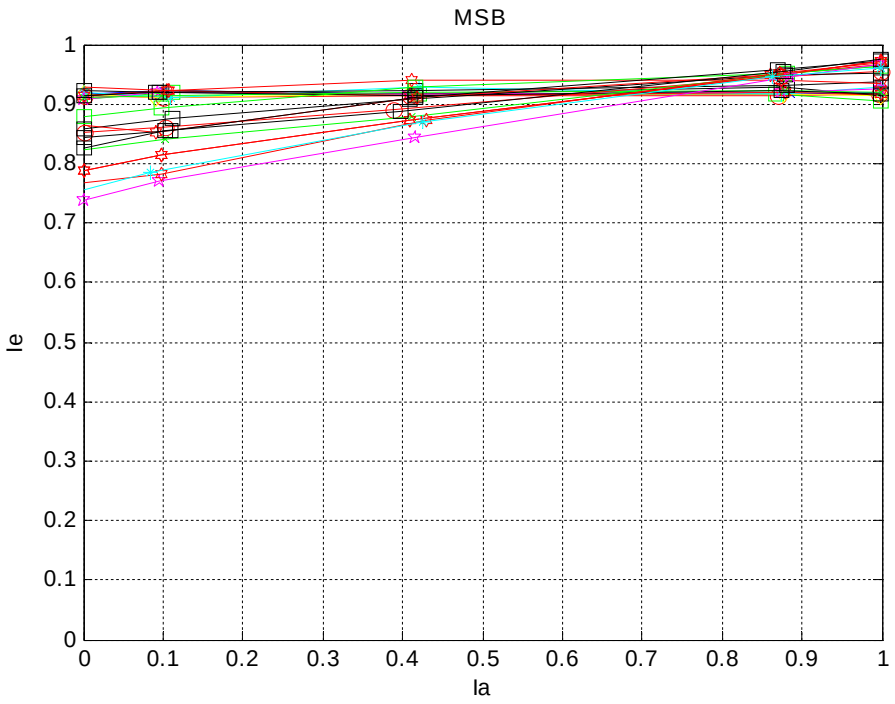

Fig.4.23 EXIT charts for first level bit (*m*=1) of random mapping 4-QAM Golden Code, *C*=3.6 bits/s/Hz, ρ=12dB, *r* = [1, 2, 5, 10, 20], $\phi = [0, \frac{\pi}{10}, \frac{\pi}{9}, \frac{\pi}{8}, \frac{\pi}{7}, \frac{\pi}{6}, \frac{\pi}{5}, \frac{\pi}{4}, \frac{\pi}{3}]$, θ=0

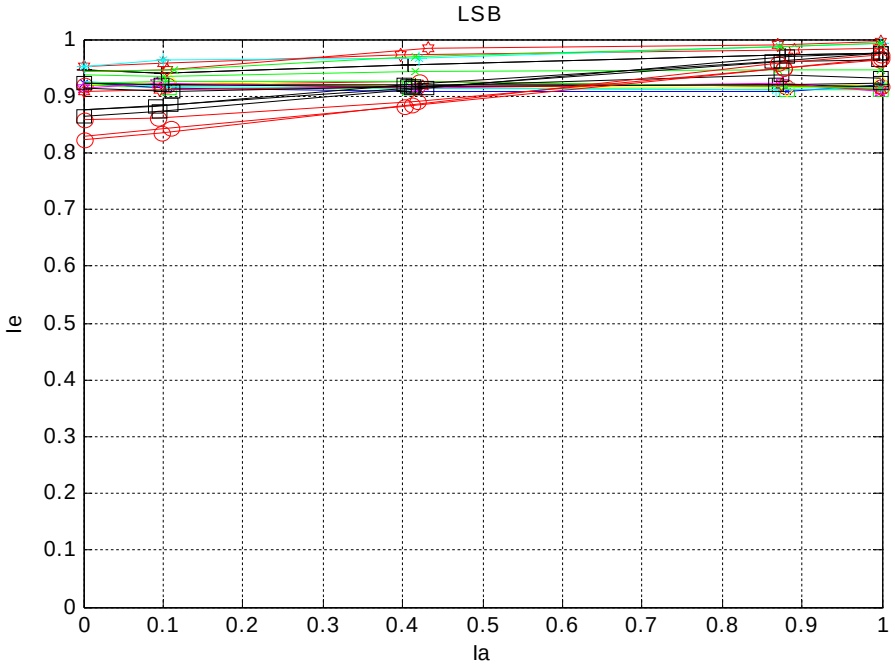

Fig.4.24 EXIT charts for second level bit (m=2) of random mapping 4-QAM Golden Code, C=3.6 bits/s/Hz, ρ=12dB, r = [1, 2, 5, 10, 20], $\phi = [0, \frac{\pi}{10}, \frac{\pi}{9}, \frac{\pi}{8}, \frac{\pi}{7}, \frac{\pi}{6}, \frac{\pi}{5}, \frac{\pi}{4}, \frac{\pi}{3}]$, θ= 0

According to the EXIT charts, the area under the EXIT curves of the first level bit (m=1) is about 0.85 and therefore, the LDPC code 1 can have rate 0.85. Similarly, the LDPC code 2 can have a rate 0.88. The total rate of this multilevel LDPC encoder is 0.865 which is not a significant improvement from the concatenated code schemes without multilevel coding.

Now we look at the case when the mapping is random and the space-time code is a 16-QAM Golden Code which makes m=4 in Fig.4.2 and Fig.4.3. The EXIT charts are shown as the following:

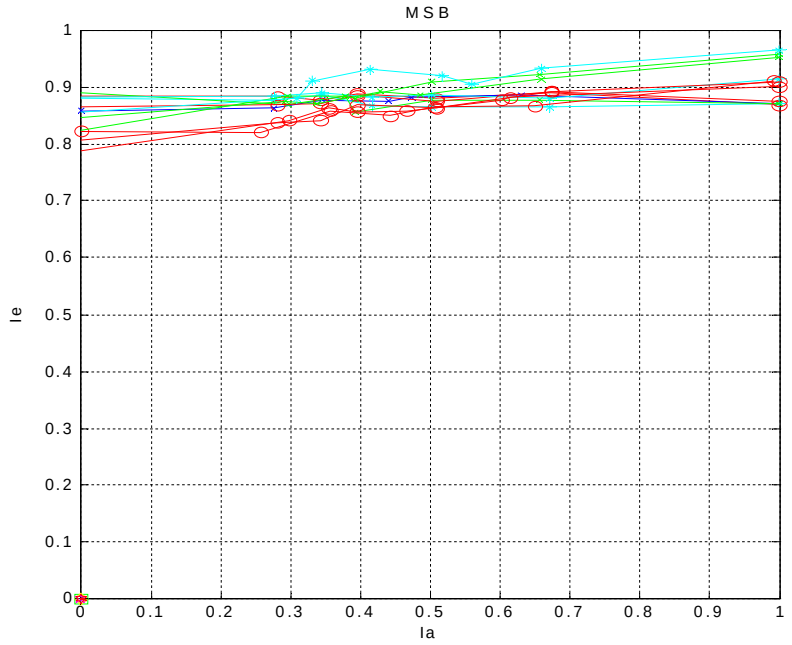

Fig.4.25 EXIT charts for first level bit (m=1) of random mapping 16-QAM Golden Code, C=7.4 bits/s/Hz, ρ=19dB, r = [1, 2, 5, 10, 20], $\phi = [0, \frac{\pi}{10}, \frac{\pi}{9}, \frac{\pi}{8}, \frac{\pi}{7}, \frac{\pi}{6}, \frac{\pi}{5}, \frac{\pi}{4}, \frac{\pi}{3}]$, θ=0

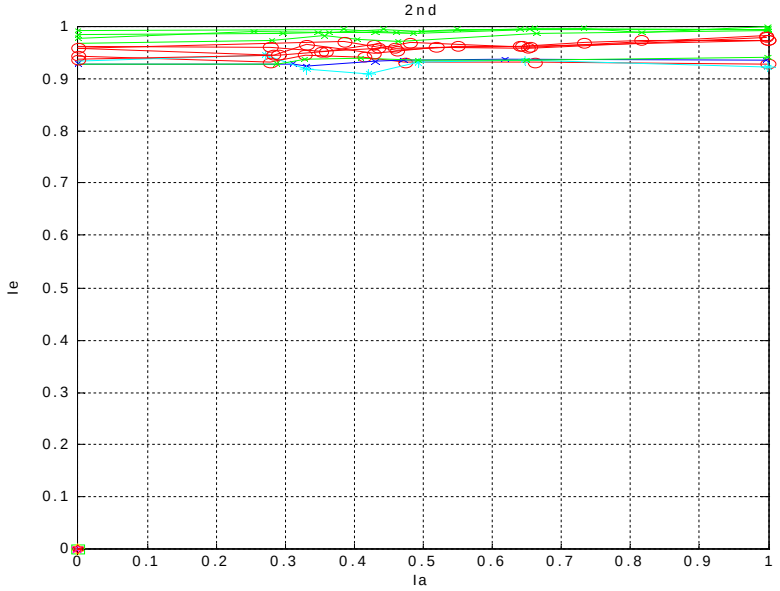

Fig.4.26 EXIT charts for second level bit (m=2) of random mapping 16-QAM Golden Code, C=7.4 bits/s/Hz, ρ=19dB, r = [1, 2, 5, 10, 20], $\phi = [0, \frac{\pi}{10}, \frac{\pi}{9}, \frac{\pi}{8}, \frac{\pi}{7}, \frac{\pi}{6}, \frac{\pi}{5}, \frac{\pi}{4}, \frac{\pi}{3}]$, θ=0

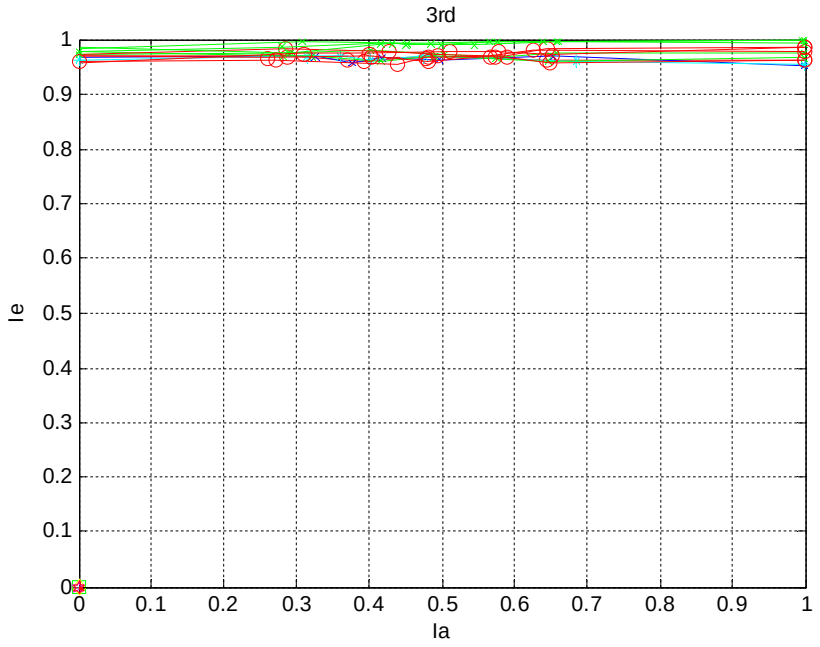

Fig.4.27 EXIT charts for third level bit (m=3) of random mapping 16-QAM Golden Code, C=7.4 bits/s/Hz, ρ=19dB, r = [1, 2, 5, 10, 20], $\phi = [0, \frac{\pi}{10}, \frac{\pi}{9}, \frac{\pi}{8}, \frac{\pi}{7}, \frac{\pi}{6}, \frac{\pi}{5}, \frac{\pi}{4}, \frac{\pi}{3}]$, θ=0

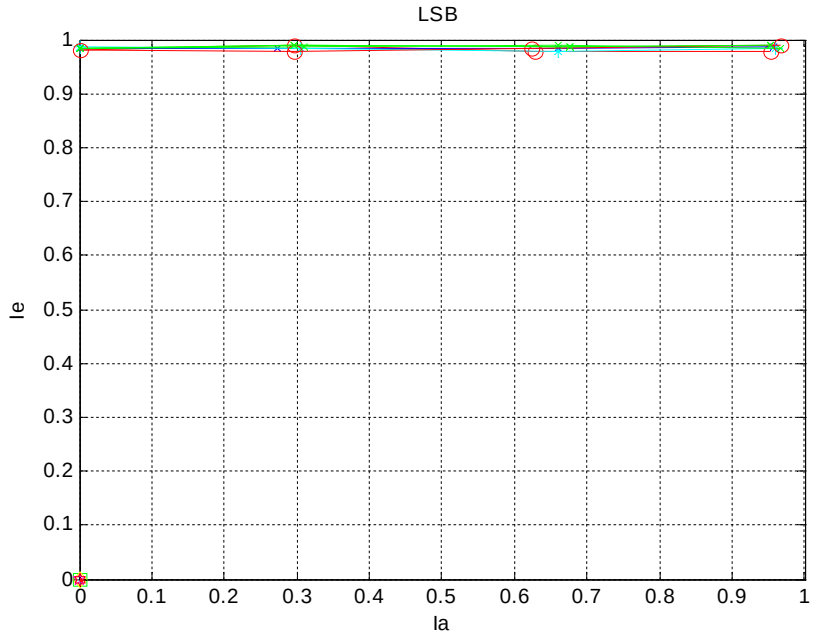

Fig.4.28 EXIT charts for fourth level bit (m=4) of random mapping 16-QAM Golden Code, C=7.4 bits/s/Hz, ρ=19dB, r = [1, 2, 5, 10, 20], $\phi = [0, \frac{\pi}{10}, \frac{\pi}{9}, \frac{\pi}{8}, \frac{\pi}{7}, \frac{\pi}{6}, \frac{\pi}{5}, \frac{\pi}{4}, \frac{\pi}{3}]$, θ=0

From these EXIT charts, the rates of LDPC codes can be concatenated with the four bits of 16-QAM Golden Code are 0.87, 0.92, 0.96 and 0.97. The total rate of the multilevel LDPC code is 0.9225 which is very close to channel capacity (0.925 bit/s/Hz at bit level). The rates of the last two bits improved significantly because of the perfect a priori information from the previous stages.

We further designed LDPC codes for each level with random mapping 16-QAM Golden Code as inner code. Notice that when gray mapping is applied, the EXIT charts for some channels are parallel to I_a axis, and the extrinsic information will not increase during the iterative process. On the other hand, when natural mapping is applied, the EXIT charts are not parallel to I_a axis, and the extrinsic information will increase during the iterative process. However, the fact that these charts have larger variation at $I_a = 0$ will cost some rate loss. Therefore, we apply random mapping so that the EXIT charts are not parallel to I_a axis, and the rate lost at small I_a can be alleviated. The EXIT charts, code rate and degree profiles of the outer codes are shown in the following:

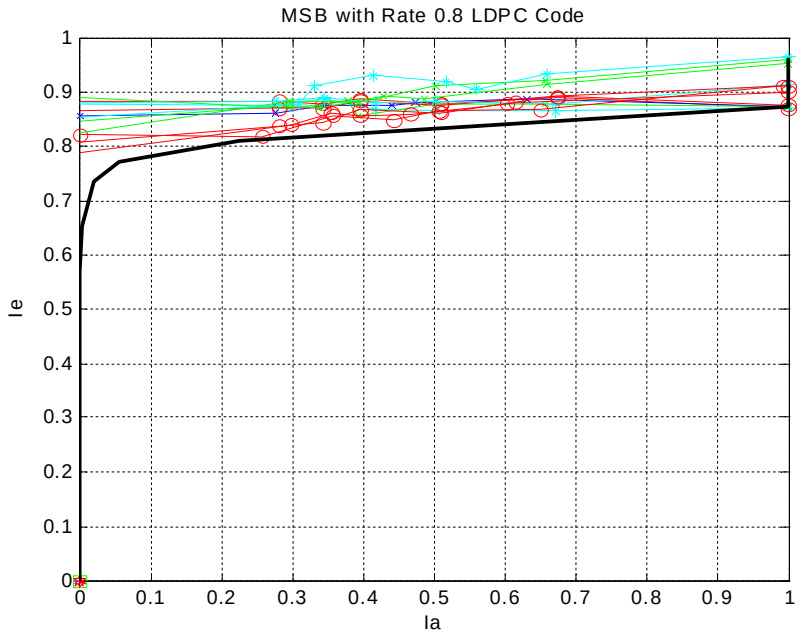

Fig.4.29 EXIT charts of rate 0.8 LDPC code ($\Lambda(x) = 0.2x^2 + 0.7x^3 + 0.1x^{11}$, $P(x) = x^{18}$) and EXIT charts for first level bit (m=1) with random mapping 16-QAM Golden Code

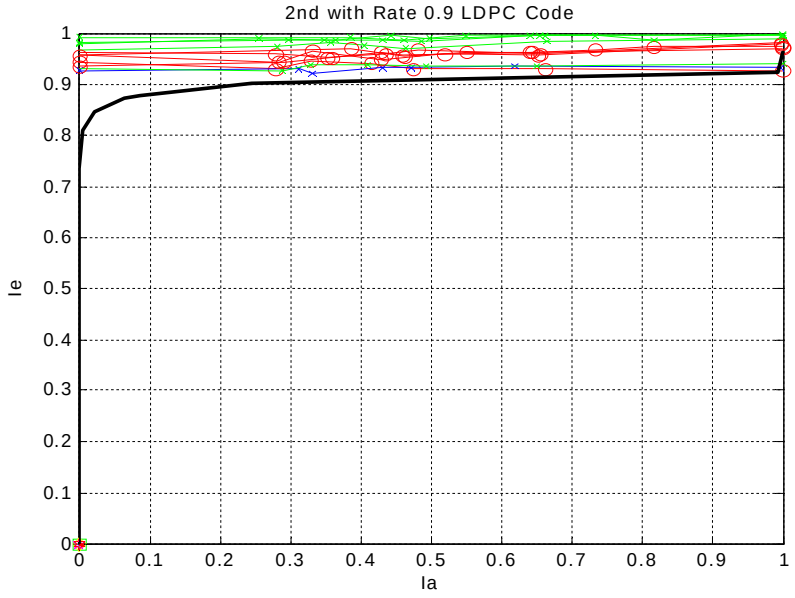

Fig.4.30 EXIT charts of rate 0.9 LDPC code ($\Lambda(x) = 0.1x^2 + 0.8x^3 + 0.1x^4$, $P(x) = x^{30}$) and EXIT charts for the second level bit (m=2) with random mapping 16-QAM Golden Code

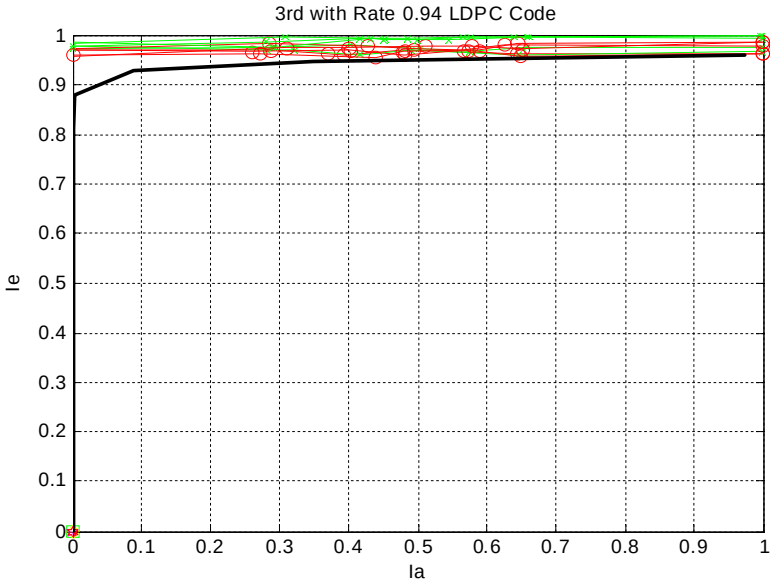

Fig.4.31 EXIT charts of rate 0.94 LDPC code ($\Lambda(x) = 0.06x^2 + 0.9x^3 + 0.04x^9$, $P(x) = x^{53}$) and EXIT charts for the third level bit (m=3) with random mapping 16-QAM Golden Code

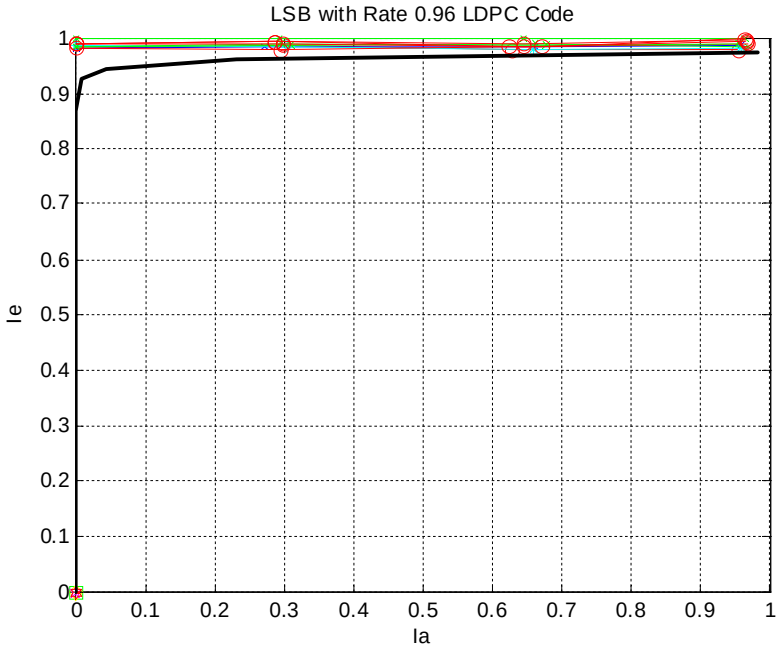

Fig.4.32 EXIT charts of rate 0.96 LDPC code ($\Lambda(x) = 0.04x^2 + 0.92x^3 + 0.04x^4$, $P(x) = x^{75}$) and EXIT charts for the fourth level bit (m=4) of random mapping 16-QAM Golden Code

4.7 Comments

Combining the results shown previously, we can design a robust serial concatenated code by using the Golden Code as the space-time modulator and an appropriate LDPC codes as the outer code. The reason is that the EXIT functions for the Golden Code show least variation over the set of channels realizations with the same capacity. Remember that our design criterion of MIMO coding is that the space-time modulator should have less variation in the EXIT functions. In other words, a good space-time code should stabilize its EXIT chart against channels. This is the most important result of this thesis. Although the rank and determinant criteria mentioned in chapter III can also be used to design a space-time code, it is the EXIT chart that provides the whole knowledge of designing a space-time code. The rank and determinant criteria only work when $I_a = 0$, therefore, cannot be directly used to understand the behavior of a space-time modulator

with iterative decoding. Nevertheless, it appears that diversity and coding are important measures of performance as the space-time codes that are optimal under these measures also seem to stabilize the EXIT functions. However, it is fully possible that space-time codes exist with better diversity and coding gains which do not stabilize the EXIT charts as well as other codes with worse coding gain or diversity, particularly for moderate to low SNRs, where the diversity and coding gain criteria may not be an accurate indicator of performance.

Applying the multilevel coding technique with Golden Code, a rate 7.2 bits/s/Hz system is designed. According to the simulation, the system has frame error rate 0.01 at ρ= 19dB in slow Rayleigh fading channel. The outage capacity Pr(C<7.4) at ρ= 19dB is 0.007. The channels that give frame error to the designed system are capacity smaller than 7.4 bits/s/Hz. Hence, the rate lost of the designed system is 0.2 bits/s/Hz.

CHAPTER V

CONCLUSIONS

The target of our work was to design a concatenated space-time code for the slow Rayleigh fading channel with no CSIT and perfect CSIR. In practice, this is usually done by concatenating an outer encoder with a space-time demodulator at the transmitter and performing iterative decoding at the receiver. The problem that we try to solve is the approach of designing the space-time code together with the outer code. Prior to this work, BICM and ML were conventional approaches to design a code for non-binary constellation. But the concatenated space-time codes designed by both approaches are not robust in slow fading channel.

In order to design a robust MIMO system, we introduce a new design approach. Based on this approach, we propose a new criterion for designing the space-time modulator and the outer code together – a good space-time code should stabilize the EXIT functions over a set of channel realizations. This new criterion considers the behavior of a space-time code with iterative decoding. The conventional design criteria of space-time code, the rank and the determinant criterion, only consider the situation when the a priori information goes into the space-time demodulator equal to zero, and do not consider the situation when a priori information is nonzero, which is important in iterative decoding.

Applying our design approach and criterion, we design a 2x2 system whose performance is close to outage capacity in slow Rayleigh fading channel and the rate lost is 0.2 bits/s/Hz. Our design approach and criterion can also apply to other MIMO systems using concatenated codes, as long as maximum likelihood decoding and the iterative decoding are performed at the receiver.

REFERENCES

[1] G. J. Foschini and M. Gans, “On limits of wireless communications in a fading environment when using multiple antennas,” *Wireless Pers. Commun.*, Vol. 6, pp. 311-35, March 1998.

[2] E. Telatar, “Capacity of multi-antenna Gaussian channels,” *Euro. Trans. Telecommun.*, Vol. 10, pp. 585-96, November 1999.

[3] E. Telatar, Capacity of multi-antenna Gaussian channels, *Eur. Trans. Telecom ETT*, vol.10, no.6, pp.585–596, Nov. 1998.

[4] L. Zheng, D. Tse, “Diversity and multiplexing: A fundamental tradeoff in multiple-antenna channels,” *IEEE Transactions on Information Theory*, Vol. 49, no. 5, pp. 1073–1096, May 2003.

[5] V. Tarokh, N. Seshadri, and A. R. Calderbank, “Space-time codes for high data rate wireless communication: performance criterion and code construction,” *IEEE Trans. Inf. Theory*, vol. 44, no. 2, pp.744-765 , March 1998.

[6] J.-C. Belfiore, G. Rekaya, and E. Viterbo, “The Golden Code: A 2×2 full-rate space-time code with nonvanishing determinants,” *IEEE Trans. Inf. Theory*, vol.51, no. 4, pp. 1432-1436, April 2005.

[7] J. –C. Guey, M. P. Fitz, M. R. Bell, and W. –Y. Kuo, “Signal design for transmitter diversity wireless communication systems over Rayleigh fading channels,” *IEEE Trans Commun.*, vol. 47, no. 4, pp. 527-537, April 1999.

[8] H. Yao, and G. W. Wornell: “Achieving the full MIMO diversity-multiplexing frontier with rotation-based space-time codes,” *Proc. of Allerton Conf. on Communication, Control and Computing* , October 2003.

[9] C. Berrou, A. Glavieux and P. Thitimajshima, “Near Shannon limit error-correcting coding and decoding: turbo codes (1),” *Proc. IEEE International Conference on Communication (ICC)*, Geneva, Switzerland, May 1993, pp. 1064-1070.

[10] J. Lodge, R. Young, P. Hoeher, and J. Hagenauer, “Separable MAP ‘filters’ for the decoding of product and concatenated codes,” *Proc. IEEE International Conference on Communication (ICC)*, Geneva, Switzerland, May 1993, pp. 1740-1745.

[11] J. Hagenauer, *Fellow, IEEE*, Elke Offer and L. Papke, “Iterative decoding of binary block and convolutional codes,” *IEEE Trans. Inf. Theory*, vol.42, no. 2, pp. 429-445, March 1996

[12] A. Ahikhmin, G. Kramer, and S. ten Brink, “Extrinsic information transfer functions: Model and erasure channel properties,” *IEEE Transactions of Information Theory*, vol. 50, no. 11, pp. 2657–2673, November 2004.

[13] S. ten Brink, “Convergence behavior of iteratively decoded parallel concatenated codes,” *IEEE Trans. On Comm.*, vol. 49, Oct 2001.

[14] R. G. Gallager, *Low-Density Parity-Check Codes*. Cambridge, MA: MIT Press, 1963

[15] J. Hagenauer, “The EXIT Chart – Introduction to Extrinsic Information Transfer in Iterative Processing,” *12th European Signal Processing Conference* (*EUSIPCO*), pp. 1541-1548, September 2004

[16] M. O. Damen, A. Tewfik, and J.-C. Belfiore, “A construction of a space-time code based on number theory,” *IEEE Transactions of Information Theory*, vol. 48, no. 3, pp. 753-760, March 2002.

[17] C. Kose, and R. D. Wesel, “Universal space-time trellis codes,” *IEEE Transactions of Information Theory*, vol. 49, no. 10, pp. 2717-2727, October 2003.

[18] D. Tse, and P. Viswanath, *Fundamentals of Wireless Communication*, Cambridge University Press, New York, 2005

[19] A. Hof, B. Baumgartner, M. Bossert and M. Weckerle, "Serially concatenated multilevel coding," *International Symposium on Information and its Applications*, ISITA2004, Parma, Italy, October 2004.

[20] S. Y. Chung, T. J. Richardson, and R. L. Urbanke, "Analysis of sum-product decoding of low-density parity-check codes using a Gaussian approximation," *IEEE Transactions of Information Theory*, vol. 47, no. 2, pp. 657-670, February 2001.

VITA

Teh-Hsuan Hsu obtained a B. En. degree in electronics engineering from National Chiao Tung University, Hsinchu, Taiwan in May 2003.

He may be reached at 1F., No.50, Cuiyi Rd., Beitou District, Taipei City 112, Taiwan. His email is hsutehhsuan@gmail.com.